COMPUTATIONAL STUDY OF THE ELECTRONIC STRUCTURE OF NITROGEN DOPED H-BOROPHENE

BY
GEZAHEGN GIZACHEW

A THESIS SUBMITTED TO THE DEPARTMENT OF PHYSICS
IN PARTIAL FULFILLMENT OF THE REQUIREMENT FOR THE
DEGREE OF MASTERS OF SCIENCE
IN
PHYSICS (CONDENSED MATTER PHYSICS)

ADDIS ABABA, ETHIOPIA
AUGUST, 2024

ADDIS ABABA UNIVERSITY
PROGRAM OF GRADUATE STUDIES

COMPUTATIONAL STUDY OF THE ELECTRONIC STRUCTURE OF NITROGEN DOPED H-BOROPHENE

By
Gezahegn Gizachew

(Department of Physics)
Addis Ababa University

Approved by the Examination Committee:

Advisor: ————————————

Dr. Chernet Amente (Associate Professor)

Examiner: Dr. Tilahun Mammo

Signature————————-Date————-/————/————

Examiner: Dr. Mesfin Birile

Signature ————————Date————-/————/————-

Chairman: Dr. Newayemedhin Aberra

Signature————————-Date————/————/————

September 7, 2024

ADDIS ABABA UNIVERSITY

September 7, 2024

Author:Gezahegn Gizachew
Title:Computational Study of The Electronic Structure of Nitrogen Doped *h*-Borophene.
Department: Department of Physics
Degree: MSc. Convocation:September Year: 2024

Permission is here with granted to Addis Ababa University to circulate and to have copied for non-commercial Purposes, at its discretion, the above titel upon the request of individuals or institutions.

Signature of Author

Dedication

This Work is dedicated to :

My Father: Thanks for always being here for me.

and

My Mother: I lost you my Great! You left fingerprints of grace on my life.
You shan't be forgotten.

and

My Wife: Tadalu Tola, I lost you my beloved! You are in my heart forever.

Acknowledgment

My sincerely thanks to all the people who have contributed to this work. First and foremost, my deepest thanks go to the almighty God, as he did much and he is always with me. I would first like, I am deeply indebted and very glad to express my sincere gratitude and appreciation to my advisor Dr. Chernet Amente(Associate Proffesor) for his important and constructive comments, criticisms and professional advice and doing all these on time from the beginning to the completion of this thesis.

I would like to express my gratitude and deep sense of appreciation to the physics department PhD students,in computational condensed matter physics, Mr. Dereje Fufa Mr.Mekuria Tsegaye ,Mr.Tamene Dechasa Dr.Tolesa Tamasgen and other friends are warmly acknowledged for their inspiration and encouragement during the research activities whenever needed. I would like to thank Addis Ababa university school of post Graduate studies and Physics department, It is also my great pleasure to thank my wife Tadelu Tola for her decision to mange my family during this work.

Finally, My special thanks goes to each and every member of my family. Words cannot express how grateful I am to my brothers Mr. Shiferaw Tola for providing both financial and moral support, which has helped me reach to this stage in life.

Contents

Acknowledgment iv
Table of Contents vi
List of Figures vii
List of Abbreviations viii
Abstract ix

1 Introduction **1**
1.1 Hexagonal- borophene and its discovery 1
1.2 Background of the study 3
1.2.1 Statement of the Problem 4
1.2.2 Objectives of the study 5
1.2.3 Significance of the study 5

2 Review Literature **6**
2.1 Conductor,Insulator and Semiconductor material 6
2.1.1 Conductor 6
2.1.2 Insulator 6
2.1.3 Semiconductor 6
2.2 Properties of Borophene 8
2.2.1 Chemical Property 8
2.2.2 Mechanical Properties Borophene 9
2.2.3 Electrical Properties 9
2.2.4 Thermal Properties 10
2.3 Application of borophene 10
2.3.1 Super capacitors 10
2.3.2 Li-S battery 11
2.3.3 Hydrogen storage 11
2.3.4 Drug delivery 11
2.3.5 Biosensor 11
2.4 Properties Nitrogen 12
2.4.1 Food Preservation 12
2.4.2 Pharmaceuticals 12
2.4.3 Manufacturing and Construction 12
2.4.4 Electronics 12
2.5 Applications of Nitrogen 13
2.5.1 Timing N Applications 13
2.5.2 Metallurgical Industry 13
2.5.3 Food Industry 13
2.5.4 Electronics Industry 13

2.6 property of *h*-BN . . . 13
2.6.1 Structural Properties and Characterization . . . 14
2.6.2 Mechanical Properties . . . 14
2.6.3 Electronic and Optical Properties . . . 14
2.6.4 Thermal Properties . . . 15
2.6.5 Toxicity . . . 15
2.7 Applications of h-BN . . . 16
2.7.1 *h*-BN in Energy Storage Applications . . . 16
2.7.2 Supercapacitors . . . 16
2.7.3 Batteries . . . 16
2.8 Semiconductors have different applications . . . 17

3 Computational methods **18**
3.1 Time-independent Schrodinger equation . . . 18
3.1.1 Born-Oppenheimer approximation . . . 19
3.1.2 The Hartree approximation . . . 19
3.1.3 Hartree-Fock Approximation . . . 20
3.1.4 Hohenberg and Kohn theorems . . . 22
3.1.5 The Kohn-Sham equations . . . 23
3.2 Density functional theory . . . 24
3.2.1 Exchange-correlation functional . . . 24
3.3 Quantum Espresso . . . 26
3.3.1 Pseudopotential . . . 26
3.3.2 Bloch's theorems . . . 27
3.3.3 Plane wave . . . 28
3.3.4 k-point sampling . . . 28
3.3.5 Band structure . . . 29
3.3.6 Density of state (DOS) . . . 30
3.3.7 Self consistency . . . 30
3.3.8 Convergence Tests . . . 31

4 Result and Discussion **32**
4.1 Geometric optimization and Electron structure of borophene . . . 32
4.2 Electronic Optimization of *h*-borophene super cell . . . 33
4.3 Electronic structure of nitrogen doped *h*-borophene . . . 35
4.3.1 Nitrogen-Doped *h*-Borophene with concentration x=0.33 . . . 35
4.3.2 Nitrogen-Doped *h*-Borophene with concentration of x=0.38 . . . 36
4.3.3 Nitrogen-Doped *h*-Borophene with concentration of x=0.44 . . . 38

5 Conclusion and Recommendation For Future Work **42**

List of Figures

2.1 The graph of conductor behavior 7
2.2 The graph of insulator behavior 7
2.3 The graph of semiconductor behavior 8

4.1 Pristine monolayer of Borophene Optimized constructed by using XcrysDen software. 32
4.2 The graph of pristine monolayer of Borophene ECUT Structure Optimization . 33
4.3 The graph of pristine k-point sampling Structure Optimization of mono layer of borophene 33
4.4 The graph of lattice parameter of borophene Optimization 34
4.5 The graph of pristine band structure of borophene 34
4.6 The graph of pristine total density of state for borophene 35
4.7 Monolayer hexagonal borophene (*h*-B) the optimized unit cell structure was replicated in x and y directions to get this $3 \times 3 \times 1$s super cell. 35
4.8 The band structure of super cell of *h*-borophene 36
4.9 The super cell of TDOS and PDOS of mono layer of *h*- B 36
4.10 The pristine of nitrogen concentration x=0.33 of *h*-borophene Optimization . . 37
4.11 The band structure at the concentration of x=0.33 nitrogen doped *h*-borophene . 37
4.12 The total density of state and the pertial density of state for the concentration of x= 0.33 of nitrogen doped *h*-borophene 38
4.13 The super cells concentration of x=0.38 nitrogen doped *h*-borophene Optimized after relaxation. 38
4.14 The band structure the concentration x=0.38 of nitrogen doped *h*-borophene . . 39
4.15 The total density of state and partial density of state concentration of x=0.38 nitrogen doped *h*-borophene 39
4.16 The super cells the concentration of x=044 nitrogen doped *h*-borophene optimization after relaxation. 40
4.17 The band structure at the concentration of x=0.44 nitrogen doped *h*-borophene 40
4.18 The total density of state and partial density of state for the concentration of x=044 nitrogen substitution *h*-borophene 41

List of Abbreviations

GGA: Generalized Geradiant Approximation

LDA: Local density approxmation

PBE: Predwe Burke Ernzerof

HF: Hartree Fock

KS: Kohn Sham

PW: Plan Wave

SCF: Self-consistence field

NSCF: Non-self-consistence field

ECUT: Energy cutoff

XC: Exchange correlation

USPP: Ultra soft pseudo potentials

PAW: Projector augmented-wave

2D h-BN: Two dimentiona hexagona boron nitride

h-BN: Hexagonal boron nitride

DFT: Density functional theory

B: Boron

N: Nitrogen

TDOS: Total density of state

PDOSE: Partial density of state

Abstract

In this study,we explore the effects of nitrogen doping on hexagonal borophene, a two-dimensional material composed of boron atoms arranged in a hexagonal structure, known for its unique electronic properties. Using density functional theory (DFT), we examine how varying nitrogen concentrations alter and enhance the material's structural and electronic characteristics. Our findings reveal that nitrogen doping induces significant changes, particularly at a concentration of x=0.38, where the band gap begins to open, transforming *h*-borophene from a metallic to a semiconducting state. As the concentration increases to x=0.44, the band gap widens, resulting in a direct band gap at the $\Gamma - \Lambda$ symmetry point. These insights suggest that nitrogen- doped *h*-borophene holds great potential for applications in transistors, photodetectors, and other electronic devices.

Keyworde:- *h*-borophene, 2D material, DFT, *h*-BN, electronic structure

Chapter 1

Introduction

1.1 Hexagonal- borophene and its discovery

Graphene is the first discovered 2D material [1]. The discovery of the very surprising properties of graphene has brought forth a series of new materials known as 2D materials [2]. 2D forms are a comparatively exciting and new area for much application. Usually, these materials have many prominent physical properties that are promising for electronic devices, nano engineering, energy conversion, and photonics. With the rapid development of graphene, 2D materials, such as phosphorene, BN, germanene, antimonene, silicene, arsenene, and transition metal dischalcogenides, have recently arisen extensive interest [3]. The research on boron in various compounds can be traced back to several hundred years ago, because boron possesses the extraordinary property to combine with nearly all of the other elements. One layer of boron atoms forms numerous crystalline shapes in this material.

Borophene is a relatively new compound. The material was initially predicted using computer models in the 1919s. But it wasn't synthesized until 2015via chemical vapour deposition. Borophene is made up of the same boron and carbon components as graphene. This critical becuause,despite their macroscopic allotropes being quite different,small atomic clusters of carbon and boron are quite similar at the nanoscale[4, 5]. To begin with borophene is stronger and more flexible than graphene which is an important attribute when considering that graphene is harder than diamond and is made entirely of carbon(one of the hardest elements that exist on the planet).

Borophene is also an electrical superconductor.The crystal structure of borophene is highly anisotropic [6]. Lots of researches foretell that different low-energy crystal structures may lead to metallic or semi-metallic behavior. its unique crystalline structure, which is created by boron atoms, is responsible for this property, since the gaps that remain between the atoms allow boron to be super-conducting[7]. Borophene's capacity to catalyze the decomposition of hydrogen and oxygen is one of its most notable advantages, it has excellent catalytic effects in the hydrogen evolution process, oxygen reduction reaction, oxygen evalution reaction and Co_2 electro-reduction reaction[8]. This might use in a new age of water based energy generation.However,scientists must complete significant amount of research before borophene usage may be considered possibility, Given that borophene's reactivity renders it susceptible to oxidation, that is still a long way to go in terms of finding a technique to generate significant amounts of material. These factors make borophene difficult to handle and expensive to manufacture, just like graphene.

It turns out that borophene is both stronger and more flexible than graphene. It also superconductors and is an excellent conductor of both electricity and heat. The characteristics of the material vary based on its orientation and the arrangement of vacancies, indicating that it is tun-able. Furthermore, borophene has the potential to be used in batteries and as a hydrogen production catalyst other issues with graphene include its mechanical rigidity which makes it unsuitable for systems that require extensive compression, stretching or torsion tolerance. Now researchers from Rice University in the United states and Nanjing University of Aeronautics and Astronautics in China report their complete first-principles analyses of the mechanical properties of borophenes in advanced functional materials.

Althougth borophene is comparable to graphene in termes of its lightness and strength it has two distant characteristics that lead to its unexpected attractive attributes. First, borophene is made up of a highly changeable horn atom network of hollow hexagons in a reference triangular lattice and its mechanical characteristics may be tailored by varying the hollow hexagon concentration. Second, due to its delocalized multicenterd bonding borophene is metallic in nature which the researchers believe might predict qualitatively novel behaviors. Among them, hexagonal boron nitride (h-BN) is a wide band gap III-V compound. It is a layered material with a graphite-like structure in which planar networks of h-BN hexagons are regularly stacked. Hexagonal-BN possesses a high chemical stability, excellent physical properties, and a high thermal conductivity [9, 10]. It is very similar to graphite, so that one may expect to prepare pure boron.

In Sands' work, the pure boron was first documented in 1957 and the bulk g-B106 with an extremely complicated structure was reported. Up to now, bulk boron is widely known to have more than 16 poly morphs, all featuring interlinked polyhedron but only a few having identified crystal structure. Borophene is a crystalline atomic mono layer of boron, it is a two dimensional allot rope of boron and also known as boron sheet. First predicted by theory in the mid-1990s, different borophene structures were experimentally confirmed in 2015 [11]. Borophene exhibit in-plane elasticity and ideal strength. It can be stronger than graphene, and more flexible, in some configurations. Boron nanotubes are also stiffer than graphene, with a higher 2D Young's modulus than any other known carbon and non-carbon nano structures[12]. Borophene undergo novel structural phase transition under in-plane tensile loading due to the functional nature of their multi-center in-plane bonding. Compared with carbon outer-shell valence electron$(2s^2 2p^2)$, boron lacks one electron with $(2s^2 2p^1)$.

Therefore, the stable configuration of honeycomb lattice of carbon is unstable for boron. Moreover, this essential difference leads to completely different structural landscape for boron. Borophene has potential as an anode material for batteries due to high theoretical specific capacities, electronic conductivity, and ion transport properties. Turning our attention to borophene, besides its interest for electronics, this new material could revolutionize sensors, batteries and catalytic chemistry[13]. Borophene has excellent possibilities as anode material for lithium-ion batteries, uses in catalysis, and its ability to detect atoms and molecules [14], [15]. Since H atoms easily stick to its surface, hydrogen storage capabilities exist. Borophene can catalyze the breakdown of molecular hydrogen into hydrogen ions, and reduce water .

2D Nano- materials have attracted major attention from the scientific community for their unique and superlative properties[11] Compared with bulk materials, ultra-thin 2D nano sheets

with the majority of atoms exposed to the surface have greater surface areas, higher 2D nano sheet chemical and physical activity, and quantum confinement effects that endow them with special photonic, electronic, catalytic, and magnetic properties, and have great application potential in bio-like materials, drug carriers, bio medicine, electronic devices, etc [16].

In 2004, the emergence of graphene led to a great response in the material field and greatly improved the applications of 2D materials in various fields [17]. However, the zero band gap of graphene hinders many applications of graphene in electronic components, biological imaging, and photo dynamic therapy. In recent years, researchers have been trying to find 2D materials with honeycomb structure like graphene, or mono elemental 2D nano sheets that are in the same group as or adjacent to carbon element, hoping to develop graphene- like materials with excellent properties. Fortunately, the emergence of the graphene like structure materials represented by transition metal sulfides ,[18] hexagonal - boron nit ride(h-BN),[19] and graphite phase carbon nitride $(g - C_3N_4)$ [20] as well as mono elemental 2D materials represented by borophene,[21] silicene,[22] stanene,[23] and germanene, can not only make up for the shortcoming of the graphene of zero band gap, but they also have some more special properties, which are expected to bring new functions and applications.

The difficult point is the analysis of electronic properties. Here we combine charge density, band structure and density of states to analyze the electronic properties. The results of scanning tunneling microscope measurements further showed that borophene is a high an isotropic metal [24], in a vast contrast to the isotropic zero gap semi-metallic graphene . Peng et al. employed First Principles calculations to study the electronic structure, bonding characteristics, as well as nitrogen doped borophene and calculate the band structures. In a word, borophene is rich in resources, has low atomic weight, is lightweight, is low cost, and has excellent electrical performances. These advantages of borophene provide it more possibilities for practical application in the future.The research on borophene is just beginning. With the development of the research on borophene, borophene not only has the above excellent properties but also may have novel atomic structure, excellent physical and chemical properties, and more interesting quantum effects, providing more possibilities for borophene-based applications in the future.

After this introduction section, the paper incorporates theory of property and application of borophene in chapter 2 computational method in section 3, results and discussion in chapter 4, conclusions in chapter 5 before future scopes and references calculation of optimizing of h-borophene. Will conclude my thesis by summarizing the results of my research work and I will discuss possible future work.

1.2 Background of the study

Semiconductors are materials with electronic properties that fall between those of an insulator and a metal. The electronic band structure of a crystalline material generally determines its electronic properties. The valence band is the highest energy band that is completely occupied by electrons, while the conduction band is the next higher-lying energy band. The distribution of electrons in a material's conduction and valence bands determines its electrical conductivity. In metals, the conduction band is partially occupied, and when an external electric field is applied, the high-energy electrons can be easily scattered into unoccupied states, resulting in good electrical conductivity.

In insulators, the highest energy electron is in the completely filled valence band, and there is no possibility of intra band electron scattering in the presence of an external electric field, leading to poor electrical conductivity. Insulators have a large energy gap, known as the band gap energy, separating the conduction and valence bands.
Semiconductors have a smaller band gap (around 1 eV) compared to insulators, which allows electrons to be excited from the valence band to the conduction band through light absorption in the visible and near-infrared regions of the electromagnetic spectrum. This property gives rise to the various interesting semiconductor applications.because semiconductor material, is a very important crucial electronic material. which is sued to apply in its application .

1.2.1 Statement of the Problem

Research in two- dimensional(2D) materials has seen a huge boost in last decade owing to strong expectations of attractive properties and exciting applications[25].Borophene is reported to have a serial marvelous nature in electronic, properties and can be a powerful competitor to graphene[6]. Borophene has certain distinctive physical and chemical properties and different phases of it have been synthesized till now. *h*- borophene, a single layer of boron, has stimulated enormous scientific interest. The interest in borophene is primarily due to its unique (unusual) properties.
It was discovered that borophene has high electronic mobility and high charge carrier concentrations, can lead to ultrahigh hydrogen storage capacity which makes borophene an interesting candidate for applications in electronic devices especially Li-S battery[26]. The borophene structure is easily accessible and it is cheap to make.Its many unique properties are still not properly understood, and need further investigations.

Similar to graphene, other 2D materials are also projected for next-generation electronic and optical devices. Hexagonal boron nitride (h-BN) is one of the promising 2D materials with superb mechanical properties, good thermal conductivity, and excellent chemical, as well as thermal stability[27] Two-dimensional h-BN, a structural analogue of graphite, in which the number of atoms of boron (B) and nitrogen (N), is it change the amount and alternatively placed . The alternate B and N atoms are connected by strong B-N bonds and 2D layers are held together by weak van der Waals forces. There is still more effort needed to understand the unique properties of this material. Hopefully, if such challenges are resolved, h-BN will find more applications in nano technology.

The primary aim of this thesis is to investigate the electronic structure of *h*-borophene and nitrogen-doped h-borophene, specifically calculating the band gap. All calculations are conducted using a pseudopotential plane wave self-consistent field simulation package within the density functional theory (DFT) framework. This study focuses on two main aspects: first, the DFT analysis of the electronic structure of h-borophene and its nitrogen-doped variant. We explore nitrogen-doped h-borophene structures with various super cell sizes to determine the structural and electronic properties of these different systems and to classify the material types. To validate our findings, we compare the calculated results with experimental data and previously published theoretical results.We are particularly interested in studying 2D material systems because of their wide-ranging interdisciplinary applications. For example, 2D h-borophen

and other emerging 2D materials offer significant potential across various fields. Additionally, first-principles computational methods have demonstrated their value in characterizing these systems, predicting new materials, and enhancing experimental efficiency. We utilize these advanced computational techniques to harness their predictive capabilities and cost-saving advantages.

1.2.2 Objectives of the study

General objectives

The aim of this study is to understand the change in electronic structure of nitrogen dopede *h*-borophene.

Specific objective

- To find the k-points sampling for the Brillouin zone of the systems and the kinetics energy cut-offs for the plane wave expansion of the wave functions.
- Determine the structural properties of the systems such as the equilibrium lattice constant and compere with the honeycomb borophene lattice parameter.
- To show how nitrogen doping affects the overall electronic band structure of *h*-borophene.
- To calculate the band gap of nitrogen doped h-borophene and the type of material.

1.2.3 Significance of the study

The study of nitrogen-doped hexagonal borophene is significant because it merges the advantageous properties of hexagonal borophene with the benefits of nitrogen doping, creating a material with highly tunable electronic, mechanical, and chemical properties. This makes it a highly promising material for a wide range of applications, including next-generation electronics, catalysis, energy storage, and quantum technologies. The ability to tailor these properties through doping allows for the development of custom materials designed for specific, high-performance applications.

Chapter 2

Review Literature

2.1 Conductor,Insulator and Semiconductor material

In order to differentiate the Conductor, Semiconductor, and Insulator, first we have to understand their extent of forbidden band i.e. separation between their conduction and valance band. The main difference between the conductor, semiconductor and insulator is in their conductivity.

2.1.1 Conductor

A conductor is a type of material that allows the electric current to flow through it i.e. it possesses least resistance in the path of free electrons. In case of conductor, the valance and conduction bands overlap. Due to this overlapping, a small potential difference across a conductor causes the free electrons to constitute electric current. All the metals are conductors Fig.2.1. The resistance of the conductors increases with the increase in the temperature. Hence, the conductor have positive temperature co-efficient of resistance. The conductors are used for making conductor wires and cables for carrying electric current.

2.1.2 Insulator

An insulator is type of material that does not allow the electric current to pass through it, due to its high electrical resistance. In the insulators, the energy gap between valance and conduction bands is very large (about 15 eV).Fig.2.2 Therefore, a very high electric field is required to push the valance electrons to the conduction band. Due to this, there are no free electrons in the conduction band. For this reason, the electrical conductivity of insulators is very low and may considered nil under ordinary conditions. At room temperature, the valance electrons of the insulator do not have enough energy to cross over to the forbidden energy gap. But, if the temperature is raised, some of the electrons may acquire enough energy to cross over to the forbidden energy gap. Hence, the resistance of the insulator decreases with the rise in temperature. Therefore, the insulators have negative temperature co-efficient of resistance. Due to high electrical resistance, the insulators are used for protection against electric shocks.

2.1.3 Semiconductor

The semiconductors are the materials having conductivity in-between conductors and insulators. In a semiconductor, the forbidden energy gap between valance and conduction bands is

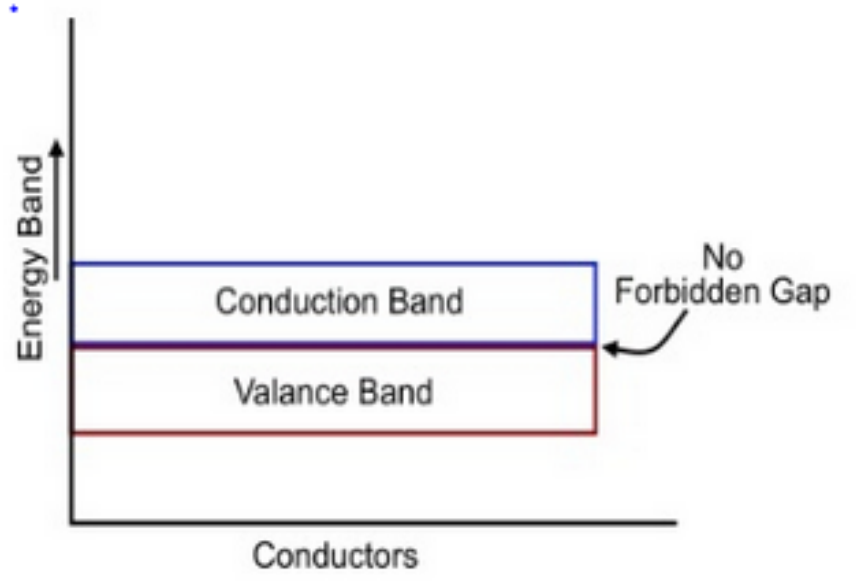

Figure 2.1: The graph of conductor behavior

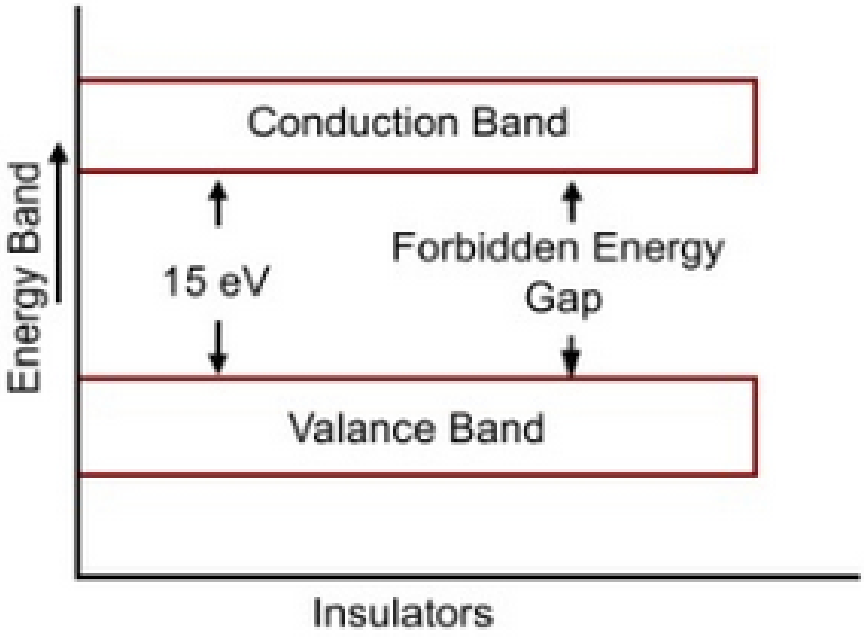

Figure 2.2: The graph of insulator behavior

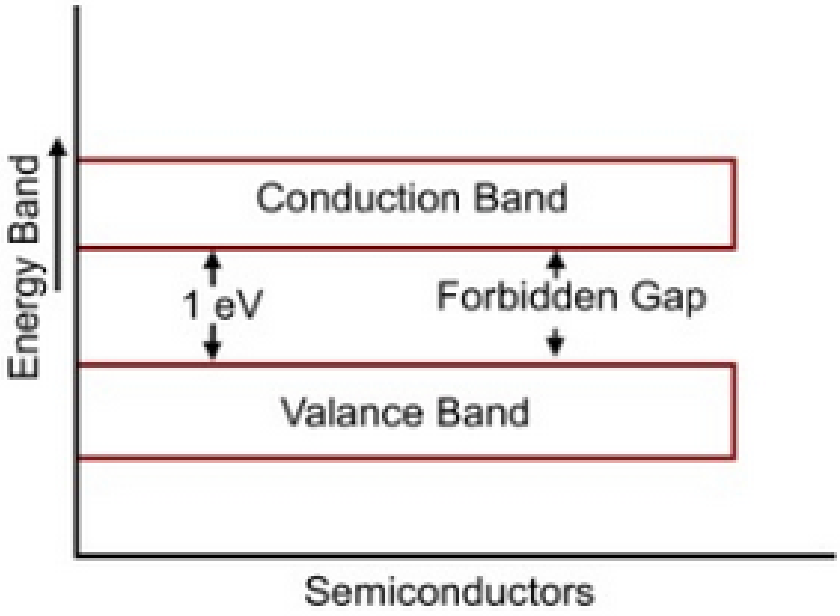

Figure 2.3: The graph of semiconductor behavior

very small (about 1 eV) as compared to insulators.Fig.2.3 Therefore, a smaller electric field (smaller than insulators but greater than conductors) is required to push the free electrons from valance band to the conduction band. At low temperature, the valance band of semiconductor is completely full and the conduction band is completely empty. Thus, a semiconductor behaves as an insulator at low temperature. However, at room temperature, some electrons can cross the forbidden energy gap, imparting a little conductivity to the semiconductor. As temperature is increased, more valance electrons cross over to the energy gap to reach to the conduction band and the conductivity increases. This shows that electrical conductivity of semiconductor increases with the rise in temperature. Hence, a semiconductor has negative temperature coefficient of resistance. The conductivity of semiconductors can also be increased by adding some impurity in the pure semiconductor material, called doping. The semiconductors are commonly used in manufacturing of solid state electronic devices.

2.2 Properties of Borophene

2.2.1 Chemical Property

The conjugations of bulk 3D boron atoms and those of 2D boron atoms around the periphery are both based on classic two-center two-electron bonds, but the inner atoms of 2D boron de localized multi center two-electron bonds, resulting in their difference in oxidation stability. In addition, (Guisinger et al.) also found that the oxidation state was detected in borophene when it was exposed to ambient conditions, yet oxidation mainly occurred on the edges of borophene because of its active edge states. Nevertheless, (Guisinger et al.) also demonstrated that borophene is not as chemically stable as other 2D materials and can be susceptible to contamination when exposed to air for long time. On the other hand, with chemical activity of borophene's edges, it can catalyze hydrogen evolution reactions; this interesting property not only providing a new possibility for the development of alternative energy, but also opening up

new pathways for the application of boron. Most of boron atoms on the surface of borophene have certain stability against oxidation. This chemical stability, while not comparable to that of graphene, helps to solve the problem of the instability against oxidation in 2D materials. Furthermore, the stability of borophene against oxygen can be increased by, for example, sealing borophene from oxygen by covering othermaterials, and they also proved that a silicon/silica oxide capping layer can greatly impede the oxidation of borophene, leading to our further study on the oxidation resistance of 2D boron.[11] On the other hand, with chemical activity of borophene's edges, it can catalyze hydrogen evolution reactions;[28] this interesting property not only providing a new possibility for the development of alternative energy, but also opening up new pathways for the application of boron.

2.2.2 Mechanical Properties Borophene

The mechanical properties of borophenr are particularly interesting and important.Firstly borophene has low mass density provided that its ideal strength and in plane stiffness are satisfactory high, borophene can be used as assist elements for designing composites. secondly, borophene is suitable for fabricating flexible nano devices because of the high standards of flexibility against off-plane deformation [29, 30]. moreover, because of the powerfully an isotropic structure in borophene, its magnetic and electronic properties can be effectively controlled for multiple applications [6]. As the boron atoms are rich in bonding configurations, borophen is polymorphic, further differentiating it from other 2D materials[31] .The low mass density of boron also results in the strong electron-phonon coupling within the scope of (10^{12})K which causes phonon-mediated superconductivity with high critical temperature. in a word borophene is rich in resources has low atomic weight is lightweight is low cost and , has excellent electrical performances. these advantages of borophene provide it more possibilities for practical application in the future. Borophene will undergo a structural phase transition at a large strain, higher mechanical thoroughness.it is the most flexible material, excellent flexibility due to its atomic thickness, with a high level of flexibility against off-plane deformation, excellent elasticity and great potential in the preparation of composite material[32].

2.2.3 Electrical Properties

The nature of electron-deficient of boron atoms makes the structural complexity of its allotropes is greater than that of carbon, leading very abundant physical properties, some of them even superior to carbon materials, such as the superconductivity and topological properties.The crystal structure of borophene is highly an isotropic. Lots of researches foretell that different low-energy crystal structures may lead to metallic or semi metallic behavior. They may include Dirac cones near or at the Fermi energy and show an isotropy of conductivity because of their isotropic bonding configuration .2D boron exhibits diversiform structural poly-morphs. Although the 2D and 3D forms of boron are alike in the organizations of chemical bonds, every 2D boron poly-morph is metallic but the nature of their 3D forms is diverse [11]

Superconductivity

Relatively low atomic mass of boron can produce strong electron-phonon coupling, and the metallicity of borophene can make itself produce a higher carrier concentration, both of which are key factors in the formation of conventional superconductors, proving that borophene has the potential to become a superconductor Nevertheless, the electron doping and tensile strain

can induce the suppression of superconductivity for borophene, [33]making it difficult for the critical temperature of borophene to be detected in experiments demonstrably. However, once these issues are addressed, these properties will increase the flexibility of design and convenience for borophene in super-conducting devices.

Semi-conductivity

Scientists have experimentally shown that several phases of borophene also have semi conductivity because of the non-zero band gaps. (Zeng et al.) Found that α and $\alpha^{'}$-sheets (slightly buckled $\alpha - sheet$) are both small-gap semiconductors with indirect band gaps of 1.40 and 1.10 eV, respectively, among which the $\alpha - sheet$ has the greatest cohesive energy and is probably the most stable buckled borophene. (Kou et al.) .Therefore,borophene has application prospects in the field of pressure-sensitive and photosensitive devices[34].

2.2.4 Thermal Properties

Have a great relationship with the structure of borophene. To eliminate the instability of borophene is to produce fully hydrogenated borophene. Special properties in thermal transport, which vary according to its structure. The phonon frequencies of various borophene phases are close to each other because borophene is composed of the same boron atom. Nonetheless, the quantities of boron atoms in each unit cell is not the same, leading to distinct geometric symmetries and different numbers of optical phonon branches, resulting in multiple thermal transport. For low frequency phonon, similar to graphene, the phonon transmission in borophene is almost isotropic, whereas for high-frequency phonon, the transmission is one-dimensional, leading to ultrahigh thermal conductivity. This indicates that the different phonon scattering rates give rise to the observed differences in thermal conductivity and thermal properties. For The special thermal properties of borophene described above provide guidance for the likely application of these materials, able to meet the different requirements of different industries. For example, high thermal conductivity can help to eliminate accumulated heat in photovoltaic and electronic equipment, while the thermometric and thermal insulation industries require low thermal conductivity materials. The multiplicity of thermal transport in borophene makes its application in thermal management and transparent conductors possible[35].

2.3 Application of borophene

A large amount of theoretical and experimental data indicated that borophene has excellent properties with potential in various applications in many fields such as super capacitors, energy storage, electronic devices, and bio-medicine, among others. The size and physio-chemical properties of borophene play a decisive role:

2.3.1 Super capacitors

Super-capacitor is a new type of energy storage device, with the remarkable properties of low cost, long cycling life, fast charge/discharge rate, high power density, and low energy density. Large, and stable voltage window On the basis of the surface charge-storage mechanism, the electrical conductivity and surface area of the electrode materials prominently affect the capacitor performance. Recent developments in 2D nano materials have afforded diversely promising candidates for super capacitors, with ultrahigh electrical mobility, extremely large surface area,

and ultra- thin thickness. And also:Good specific capacitance, Excellent rate capability, Good cycling stability, Excellent energy density[36].

2.3.2 Li-S battery

The advance of lithium-sulfur batteries has been hampered by the fast capacity fading induced by the shuttle effect. Suitable sulfur anchoring materials can suppress the shuttle effect and improve the cycling performance. The interaction between the anchoring material and lithium polysulfides should not be too strong or too weak. As for graphene, the adsorption energies of $\hat{L}i_2s_4, Li_2S_6 and Li_2S_8$ 0.65, 0.72 and 0.73 eV, respectively. Due to the weak interaction, graphene is not a suitable anchoring material for lithium polysulfides. It is imperative to search for more suitable anchoring materials for lithium batteries. The application of borophene as the potential anchoring materials for lithium-sulfur batteries has been studied by first principles calculations[26]. The suitable adsorption strength is helpful to suppress the shuttle effect and keep their cyclic structure undecomposed during the charging and discharging processes. Furthermore, borophene shows a metallic electronic structure during the whole battery cycling.

2.3.3 Hydrogen storage

As the lightest 2D material, borophene is also a promising material for hydrogen storage, and can lead to ultrahigh hydrogen storage capacity. For the sheet of borophene, the adsorption energy of a single H_2 molecule is only 0.047 eV. The interaction of H_2 molecule with the-sheet phase of borophene shows similarities to its interaction with graphene (0.025 eV)[37].The adsorption energy is too small for practical hydrogen storage. Metal atom decoration is an effective and feasible approach to strengthen the interaction. After Li decoration of -sheet phase of borophene, the adsorption energy of H_2 molecule reaches 0.35 eV, a significant increase compared to that without the Li decoration.

2.3.4 Drug delivery

The localized release of chemotherapeutic drugs is the key to reduce the side effects of chemotherapy. Therefore, it is especially important to design a smart tumor micro environment response drug-release platform. The ultrahigh specific surface area of borophene provides space for drug loading and anchor points for functional group modification, making it a suitable material for many aspects of anti-cancer treatment. borophene with high drug loading capacity and pH and infrared dual response, is a promising integrated drug delivery platform for both the diagnosis and treatment of cancer[38].

2.3.5 Biosensor

In the biomedical applications of nano- materials, borophene is often used as a 2D nano material combined with other metals and semiconductor materials to improve the performance of biological applications without any negative effects. DNA sequencing has been realized by different methods through the determination of base sequence, which has a great impact on the decoding of human biological code. However, the application of nano materials in this technology will greatly accelerate the research of biology and medicine .Thus, borophene nano sheets could be used in biological DNA sequencing devices. Borophene is efectively used for biosensors. By testing the energy and electron sensitivity of 2D borophene to the four bases (adenine

(A), guanine (G), thymine (T), and cytosine (C)) on top of biological DNA, the scientists found that different bases attached to borophene produce different conductivity, resulting in different electrical signals. In addition, Das et al. also measured the sensitivity of borophene to different bases,$A > G > C > T$[39]

2.4 Properties Nitrogen

Nitrogen, the seventh most abundant element, is a colorless, odorless and nonreactive gas that makes up about 80% of our atmosphere. This chemical element is almost everywhere we look and has a ton of different uses, such as preserving food and making common medicines in the pharmaceutical industry. At nexAir, we will continue to use our years of industry experience and Know how in order to educate our customers and employees on all of the products and services that we offer – gases included. While nitrogen has many different uses, here's four that we think are important:

2.4.1 Food Preservation

One of the most common usages of nitrogen is in the food industry for packaging. This gas allows the foods to stay fresh by preventing oxidative damage, leading to spoilage. The nitrogen creates a man-made atmosphere for the food items to keep fresh and reduces the chances of the food going bad before it gets to its final destination.

2.4.2 Pharmaceuticals

Did you know that nitrogen gas is present in every major drug class? Nitrogen gas is actually widely used in the pharmaceutical industry including antibiotics and anesthetics. This may be a lesser-known fact, but nitrogen can also be used to preserve biological specimens.

2.4.3 Manufacturing and Construction

Nitrogen can also be used during a process called "shrink fitting", where the inner part of the metal is cooled by using liquid nitrogen, further making it shrink. Another common use of nitrogen is in the construction industry for tunnel construction. This process consists of pumping the liquid nitrogen through pipes, and once the nitrogen is deposited through the soil, it vaporizes – eliminating the heat and freezing it.

2.4.4 Electronics

This may be surprising to some, but nitrogen plays a pretty big role in the electronics industry. Nitrogen is typically used in the manufacturing and production of electronics, to create an inert atmosphere while preventing oxidation. This gas helps to prevent any kind of electrical failure or issues that could potentially arise.

2.5 Applications of Nitrogen

2.5.1 Timing N Applications

The goal of timing nitrogen (N) applications to corn is to supply adequate N when the crop needs it, without supplying excess that can potentially be lost. Because N reactions in the soil are closely linked to both temperature and moisture conditions, this goal is often hard to achieve. Its importance, however, cannot be overstated. If corn is deficient in N during its rapid vegetative growth phase, yield losses are inevitable. On the other hand, oversupply of this expensive crop input reduces profits and harms the environment. Applying N at multiple times, including the time of maximum crop uptake, can spread the risk of N loss and crop deficiency, improve profitability by reducing N rates, and benefit the environment.

2.5.2 Metallurgical Industry

In different chemical reactions, either in industry or in laboratory, an oxygen-free atmosphere is essential to obtain the desired product. Moreover, liquid nitrogen is widely used for the cooling of scientific equipment, for the cryopreservation of biological samples and for many other processes. Nitrogen is used also in the plastic industry for the production of expanded polymers and for gas-assisted injection moulding.

2.5.3 Food Industry

Nitrogen is widely used, either pure or in a mixture, in the preservation of industrial foodstuffs, as main component of a protective atmosphere. Mixtures particularly rich in nitrogen are used in the protection of foods where unsaturated fats are present in significant quantities, to eliminate oxygen and avoid rancidity.

2.5.4 Electronics Industry

In the production of electronic components such as transistors, diodes and integrated circuits, nitrogen is used either as a carrier gas of process gases and for the creation of inert atmospheres during heat treatments.

2.6 property of *h*-BN

Well-known for its exceptional physicochemical and mechanical properties, *h*-BN possesses interesting dielectric, mechanical, and thermal properties suited for numerous applications.[40] *h*-BN forms a hexagonal lattice with strong in-plane polar bonds between B and N, typically characterized by several optical microscopic and spectroscopic techniques. The type and concentration of intrinsic defects, doping, and functionalization of*h*-BN can change the electronic properties of *h*-BN completely. Dopants and defects create additional states that could introduce emergent properties such as magnetism and single-photon emission. he edge termination of the *h*-BN flakes, nanowires, nanotubes and nano ribbons also critical in determining overall band gap and chirality.

2.6.1 Structural Properties and Characterization

Individual *h*-BN monolayers form a honeycomb lattice with alternating boron and nitrogen atoms covalently bonded to each other with a bond length of $(1.45A^o)$, with a separation of $(2.5A^o)$ between the neighboring rings. Structural properties of different morphologies of BN can be distinguished by the plethora of characterization techniques. An easy way to estimate the number of layers in the 2D *h*-BN is optical microscopy; where the amount of light absorption can be used to derive the number of layers by calculating the step height with respect to the surface. However, this only works for 2D *h*-BN due to its resolution limitations $\approx 1micrometer$ .For other types of morphologies such as BNNS or *h*-BN nano ribbons, atomic force microscopy (AFM), and scanning electron microscopy (SEM) are beneficial resolution.AFM can also be used to measure the mechanical properties of *h*-BN; described in detail in the mechanical properties section. The most common technique to determine the structure of the *h*-BN is X-ray diffraction (XRD). In recent years, Raman spectroscopy also has been frequently used to identify the number of layers with the help of in-plane phonon mode in the range $1364 - 1371cm^{-1}$. For a mono layer, the Raman peak broadens and shifts to a higher wave number of $1370cm^{-1}$ as compared to the bulk peak at $1366cm^{-1}$ serving as a standard to indicate BNNS presence due to the red shift. All these techniques are non-destructive and easy to perform but are limited by an optical resolution limit.[41]

2.6.2 Mechanical Properties

The mechanical properties of *h*-BN can be theoretically calculated by Density Functional Theory (DFT) and/or Molecular Dynamics (MD) simulations and experimentally determined by in situ techniques based on SEM, Transmission Electron Microscopy (TEM), AFM, and/or micro-electro mechanical systems (MEMS) devices. It should be noted that the mechanical properties can vary due to defect density, morphology, and thickness of the material.

DFT calculations to show that the grain boundaries (GBs) affect 2D *h*-BN sheets such that homo elemental bonds could modulate the atomic structures and stability of the *h*-BN sheet, and the formation energy to the mis orientation angle features a downward opening parabolic relationship. Similar to defects, Young's modulus is also affected by the thickness of *h*-BN. Kim et al. measured the mechanical strength in a multilayer *h*-BN film of thickness 15 nm . Thomas et al. used classical molecular dynamics to investigate system size dependenc on the mechanical stability, bending stiffness, and elastic properties and concluded that a direct relationship existed between system size and Young's modulus. An increase of the Young's modulus also meant an increase in wave velocities in both the longitudinal and shear modes, with finite sheets displaying anisotropic behavior whereas infinite sheets are naturally isotropic in behavior. Though Young's modulus of *h*-BN is predicted to be isotropic, the fracture strength and strain are anisotropic.[42]

2.6.3 Electronic and Optical Properties

Due to this anisotropy, a large range of fracture strength values (68–215 GPa) are reported. Similar to Young's Modulus, the fracture strain and strength of such a system show an inverse relationship with the sheet thickness; with decreased sheetthickness comes increased bending moduli. Band gap and Its Tun ability: Due to the large electronegativity difference between B and N; *h*-BN acts as an insulator with a wide band gap. Usually the band gap of *h*-BN is characterized by photoluminescence (PL) and optical absorption. Early theoretical calculations

on the band gap of *h*-BN produced a band gap range of 3.9–4.6 eV, although experimental data show much higher values. Recent in-depth studies have established that the band gap of 2D *h*-BN is generally around 6 eV, with an indirect band gap of 5.95 eV for its single crystal, and a direct band gap of 6.1 eV for monolayer *h*-BN. Despite being an optically transparent material due to its low absorption in the 250–900 nm wavelength range,[43] *h*-BN exhibits an exceptionally high absorption peak in the deep UV range (200–220 nm) due to its anisotropic structure, further indicating the presence of a direct band gap in *h*-BN. Also, it is observed that the fundamental electronic property of *h*-BN is highly dependent on the fabrication strategy.Koch et al. investigated the differences in the electronic properties of epitaxial in situ grown *h*-BN in contrast to exfoliated bulk *h*-BN flakes.

It is found that the valence bandwidth and the band separations of both varied substantially, on the scale of electron volts. The epitaxial *h*-BN displayed significantly reduced bandwidth compared to the exfoliated bulk *h*-BN flakes which had a full valence band electronic structure resembling theoretical predictions from GW calculations. Another interesting observation is the correlation between electronic structure and energetics of *h*-BN nanoribbons due to edge termination. Although its wide band gap primarily renders *h*-BN as an insulator, exceptions (e.g., zigzag *h*-BN nanoribbons) can exhibit a semi-metallic behavior. Yamanaka and Okada explained the relation between the physical properties of hydrogenated and pristine *h*-BN nanoribbons. When the edges are hydrogenated, the formation energy is found to be constant for all edge angles from armchair to zigzag.[44]

2.6.4 Thermal Properties

The extraordinary thermal properties of the *h*-BN are due to the covalent bonding between each boron and nitrogen atom. Weak vdW forces allow the layer of BN sheets to be easily sheared apart with methods such as compounding and mixing. With high-temperature stability and a melting point of around $2600c^0$, *h*-BN also theoretically has a low density of $2.27gcm^{-3}$. The in-plane thermal conductivity of *h*-BN is theoretically calculated to be more than $600wm^{-1}k^{-1}$at room temperature using the phonon Boltzmann transport equation, while its bulk counterpart is $400wm^{-1}k^{-1}$.[11] With a wide band gap of about 6 eV, atomically thin *h*-BN is in sensitive to thickness change, making it versatile, allowing flexibility for potential use as strong, electrically insulating material. One-atom thick, high-quality *h*-BN has an in-plane thermal conductivity value of $751wm^{-1}k^{-1}$ at room temperature. Thermal conductivity in BN can be measured either in or through the plane, taking into account the dissipation mechanism or the heat transfer mechanism, respectively.A nanosecond laser-based transient thermo reflectance (TTR) technique can be used to measure the in-plane and out-of-plane thermal conductivity of h-BN; the high in-plane thermal conductivity coupled with atomic flatness puts this material in the limelight for innovative thin-film devices.

2.6.5 Toxicity

Because of its use in cosmetics as a filler (slip modifier), the toxicity of *h*-BN is well studied and a recent summary in 2015 deems it safe for use. They noted that at a 50% concentration, BN caused minimal irritation, at 18.7%, it is not a sensitizer and in a 2-week use study, a cosmetic makeup containing 13%BN did not cause any adverse effects. An interesting study on the toxicity of BN nanomaterials conducted in 2017 on a worm (whole-body animal model) noted that highly soluble BN powder was more toxic (produces more reactive oxygen species

aka ROS) than hydrophobic BN nanosheets.

2.7 Applications of h-BN

Some of the most prominent applications of *h*-BN have been discussed in the following section.

2.7.1 *h*-BN in Energy Storage Applications

For 2D applications like electrochemical energy storage, *h*-BN is an isoelectric analog of graphite that has been widely commercialized as Li-ion battery anodes. However, the poor electrical conductivity of *h*-BN makes this material electrochemically inactive unless the structure is fundamentally altered, or composites of *h*-BN are fabricated involving a conducting matrix. On the other hand, the insulating nature and mechanical strength of *h*-BN are highly attractive for energy storage devices due to their capability to act as a part of a separator or an additive to the electrode, especially for highly demanding environments. However, facile functionalization, structural modification, and integration into composites have facilitated the use of *h*-BN in energy storage devices such as supercapacitors, and rechargeable lithium battery systems,

2.7.2 Supercapacitors

The utilization of pristine *h*-BN has been limited only to traditional dielectric capacitors owing to its wide bandgap (≈5 eV) as compared to the prevalent supercapacitor materials. Semiconductor materials research has shown that doping or forming composites with graphene can increase the electrical conductivity for *h*-BN, making it suitable for super- capacitor applications. In this regard, Saha, et al. reported a composite comprising graphene/*h*-BN with a super lattice structure and exhibits a specific capacitance of $8241 Fg^{-1}$ due to contributions from both double-layer capacitance and pseudocapacitance. The electrochemical activity of *h*-BN upon forming a composite with conductive matrix possibly originates from altered oxidation state of N, which is ionically bonded to B atoms. The incorporated *h*-BN nanosheets act as a super-highway for ion transport in gelpolymer electrolytes,resulting in a quasi-solid-state supercapacitor, that can deliver a high specific capacitance of $124.5 Fg^{-1}$and stable over 5000 charge–discharge cycles.[45] In most literature, *h*-BN plays either the role of an electrode composite with conductive materials or supercapacitor applications, or that of an additive to the electrolyte, which can be used for the fabrication of devices with multidimensionality, flexibility, and suitable highly demanding environments.[46]

2.7.3 Batteries

h-BN also finds its potential application in batteries for Li-ion intercalation owing to its structural similarities to graphite (standard battery anode). There are a few studies on the intercalation chemistry of lithium with *h*-BN, although it is an electrical insulator. Though the exact phase or concentration of Li in h-BN cannot be pinpointed, the Li-ion intercalation canoccur at the defective sites of *h*-BN. Chemically synthesized lithiated *h*-BN compounds are thermally more stable than lithiated graphite compounds. First-principle computations have predicted that the heterostructure of *h*-BN and blue phosphorene could be a potential anode for Li/Na batteries where Li-ions occupy interlayer sites in the heterostructure, whereas Na is preferentially adsorbed on the phosphorene layer. However, a composite polymer film with *h*-BN

delivers much better safety by providing an ion-conducting pathway, along with a thermally and chemically stable structure to maintain the electrode separation. Besides enabling the structural framework, exploration of unique *h*-BN nanostructures to produce ionic solutions and quasi-solid electrolytes also provide exciting new avenues. Hence *h*-BN is an intriguing material with immense potential to develop high-performance energy storage devices such as supercapacitors and lithium batteries with greater dimensionality control, mechanical security, and thermal stability. Conventional polymer-based separators, acting as physical barriers that prevent electrical contacts between electrodes, often face safety issues when Li-ion batteries overheat and/or overcharge.[47]

2.8 Semiconductors have different applications

Also each with a different purpose or advantage.

- Diodes :allow current to flow in only one direction, commonly used in power supplies and lighting applications.
- Transistors: act as switches or amplifiers and are a fundamental building block of digital electronics.
- Microprocessors:are ICs that contain a CPU, memory, and other circuitry and are the brain of many electronic devices such as computers, smartphones, and home appliances.
- Solar cells: convert sunlight into electricity and are made of semiconductor materials like silicon.
- LED lights: are semiconductor devices that emit light when a current is applied and are used in lighting applications.

Chapter 3

Computational methods

3.1 Time-independent Schrodinger equation

To simulate a composite system consisting of N interacting electrons and M nuclei, the many-body wave function $\psi(r_i, R_i)$ is used to describe its quantum state. This wave function ψ depends on the electronic coordinates r_i and the nuclear coordinates R_i and is the solution of the time-independent Schrodinger equation. Its non-relativistic form can be written as:

$$\hat{H}\Psi(r_i, R_i) = E\Psi(r_i, R_i) \tag{3.1}$$

With: $\hat{H}$: Hamiltonian operator E: total energy of the system Ψ: wave function
The Hamiltonian is written as:

$$(\hat{T}_{ee} + \hat{T}_{nn} + \hat{T}_{en} + \hat{T}_{ne} + \hat{V}_{en} + \hat{V}_{ee} + \hat{V}_{nn} + \hat{V}_{ne})\psi = E\hat{\psi} \tag{3.2}$$

where Kinetic energy of electrons

$$\hat{T}_e = -\sum_{i=1}^{N} \frac{\hbar^2 \nabla_i^2}{2m_e} \tag{3.3}$$

Kinetic energy of the nuclei

$$\hat{T}_n = -\sum_{i=1}^{M} \frac{\hbar^2 \nabla_i^2}{2M_n} \tag{3.4}$$

Attractive energy between electrons and nuclei

$$\hat{V}_{ne} = -\sum_{i=1}^{M}\sum_{j=1}^{N} \frac{Z_i e^2}{|R_i - r_j|} \tag{3.5}$$

Repulsive energy between electrons

$$\hat{V}_{ee} = \frac{1}{2}\sum_{i=1}^{N}\sum_{j>1}^{N} \frac{e^2}{|r_i - r_j|} \tag{3.6}$$

Repulsive energy between nuclei

$$\hat{V}_{nn} = \frac{1}{2}\sum_{i=1}^{M}\sum_{j>1}^{M} \frac{Z_i Z_j e^2}{|R_i - R_j|} \tag{3.7}$$

with
N: number of electrons
M: number of nucleus atom
r_i: electronic coordinate
R_i: nuclear coordinate
M_n: mass of the nucleus
Z_i: atomic number of the nucleus
m_e : mass of electron
Hence,
The Schrodinger equation can be written as:

$$E\Psi = \Bigg[-\sum_{i=1}^{N} \frac{\hbar^2 \nabla_i^2}{2m_e} - \sum_{i=1}^{M} \frac{\hbar^2 \nabla_i^2}{2M_n} - \sum_{i=1}^{M} \sum_{j=1}^{N} \frac{Z_i e^2}{|R_i - r_j|} + \frac{1}{2} \sum_{i=1}^{N} \sum_{j>1}^{N} \frac{e^2}{|r_i - r_j|} + \frac{1}{2} \sum_{i=1}^{M} \sum_{j>1}^{M} \frac{Z_i Z_j e^2}{|R_i - R_j|} \Bigg] \Psi \tag{3.8}$$

Although the Hamilton operator is known, Eq. (3.2) is too complex to be solved due to the large number of variables the wave function ψ(r) depends on. First step in simplifying Eq. (3.2) is to use same approximation:

3.1.1 Born-Oppenheimer approximation

Since the nuclei are much heavier than the electrons it is assumed within the Born-Oppenheimer approximation, that the response of the electrons to an external perturbation is much faster than the response of the nuclei. Thus, the electrons would be able to follow any movement of the nuclei quasi instantaneously and might then be considered as basically moving in a constant field generated by the nuclei at fixed positions. The kinetic energy term T_N for the nuclei in Equation (3.4) is set to negligible, it is much Mach small and the repulsion term for the nuclei,V_{NN} , enters the total energy as a constant and therefore, with help of this first approximation the electronic Schrodinger Equation (3.2) is reduced to,

$$\hat{H}_{tot}\Psi = \left(\hat{T}_e + \hat{V_{ee}} + \hat{V_{ext}} \right) \psi(r_i) = E_{tot}\Psi \tag{3.9}$$

With the electronic Hamilton operator $\hat{H}_e$, the electronic wave function$\psi_e(r_i)$ and the electronic energyE_e ,Equation (3.8) is simple compared to Equation(3.2).However, solving Schrodinger equation is very difficult to solve for more than 2 electrons ,hence to handle this we need further approximation[48].

3.1.2 The Hartree approximation

Hartree introduced in 1927 a procedure, which he called the self-consistent field method, to approximate the Schrodinger equation. The simplest approximation is multi electron system is the Hartree approximation. Accordingly, the electron wave function in Equation (3.9) can be approximated as

$$\psi_e(r_1, r_2, ..., r_N) \approx \psi_e(r_1)\psi_e(r_2)...\psi_e(r_N) \tag{3.10}$$

That is, swapping any fermion for any other fermion should result in the wave function remaining unchanged except for a change in sign. As any pair of fermions with the same quantum numbers approaches each other, any wave function with that property will tend to zero (indicating zero probability). Because the Hartree product wave function is symmetric rather than antisymmetric (it remains exactly the same after the interchange of two fermions), the Hartree approach effectively ignores the Pauli exclusion principle. From which allows that the electron are independent and interact only via the mean field coulomb potential resulting from ion electron interaction. One of the Schrodinger equations of the from

$$\left(\frac{\hbar^2\nabla^2}{2m_e} + V_{eff}(r)\right)\psi(r_i) = E_i\psi(r_i) \tag{3.11}$$

Where V(r) is the potential in which the electron moves this includes both the nuclear electron interaction

$$V_{ne}(r) = -e^2\sum_{R}^{ne}\frac{1}{|r-R|} \tag{3.12}$$

And the mean field arising from the N-1 other electrons. This other electrons are means out in to a smooth negative charge density n(r') leading to a Hartree potential in the form of

$$V_e(r) = -e\int dr' n(r')\frac{1}{|r-r'|} \tag{3.13}$$

Where total electron density is given by

$$n(r) = \sum_{i}^{occ}|\psi(r_i)|^2 \tag{3.14}$$

In the equation3.14 the sum over all occupied states. While this functional form is fairly convenient. It has at least one major short coming. It fails to satisfy the anti-symmetric principle. Which states that a wave function describing fermions should be anti-symmetric with respect to the interchange of any set of space -spin coordinator.

3.1.3 Hartree-Fock Approximation

Hartree- Fock theory was developed to solve the electronic Schrodinger equation that results from the time- independent Schrodinger equation after invoking the Born-oppenheimer approximation. A possible consistent Ansatz is to construct the many-body wave function as a product of (normalized) individual wave function then

$$\psi(r_1,..,r_N) = \varphi_1(r_1)\varphi_2(r_2)...,\varphi_N(r_N) \tag{3.15}$$

This Anstaz is known it leads to the Hartree method, not in use any more because it neglects an important property of electrons that they are Fermi particles, and the wave functions of a system of fermions must be anti-symmetric with respect to interchanging any pair of particles.

$$\psi(r_1...r_k,...r_\ell,...r_N) = -\psi(r_1,...r_\ell,...r_k,...,r_N) \tag{3.16}$$

We emphasize here that the position of an argument in ψ fixes the number of particular electron, and the argument value the actual coordinate of that electron, obviously, enough the wave function constructed according to (3.15) does not possess this property. Actually, it does not have any particular symmetry property. With respect to interchanging particles, but we can easily force the wave function to obey Equation (3.16); for this, we simply the products like (1), interchange these position of all particles pairwise and construct the combinations which are a priori anti-symmetric. This is easy to do for two particles.

$$\psi(r_1, r_2) = \frac{1}{\sqrt{2}}[\varphi_1(r_1)\varphi_2(r_2) - \varphi_1(r_2)\varphi_2(r_1)] \tag{3.17}$$

The factor $\frac{1}{\sqrt{2}}$ is introduced in order to keep the normalization. If our one-particle wave functions are normalized to 1, i.e.the probability to find one electron some, where in space

$$\int |\psi(r)|^2 dr = 1 \tag{3.18}$$

Then the probability to find two particles anywhere in space must be 1, and indeed

$$\begin{aligned}\int |\psi(r_1, r_2)|^2 dr_1 dr_2 = \frac{1}{2}\Bigg\{ & \int |\varphi_1(r_1)|^2 dr_1 \int |\varphi_2(r_2)|^2 dr_2 \\ & - \left[\int \varphi_2^*(r_1)\varphi_1(r_1) dr_1\right]\left[\int \varphi_1^*(r_2)\varphi_2(r_2) dr_2\right] \\ & - \left[\int \varphi_1^*(r_1)\varphi_2(r_1) dr_1\right]\left[\int \varphi_2(r_2)\varphi_1(r_2) dr_2\right] \\ & + \int |\varphi_2(r_1)|^2 dr_1 \int |\varphi_1(r_2)|^2 dr_2 \Bigg\} = 1\end{aligned} \tag{3.19}$$

In doing so, we assumed that individual one particle wave function is orthogonal. This is indeed the case if they are solution of the same Hamilton operator. If they are not for some reason but still form the complete basis of solutions to the corresponding one-particle problem, they can be one by one orthogonalzed before proceeding further with the construction of the many-body wave function. There are N! Possibilities to interchange them.

We sum up over all of them, try all possibilities to interchange every two electrons and write down anti-symmetric terms like in Equation(3.17). This results in a fully anti-symmetric wave function. It is common and convenient to write down the wave functions as determinants, because it is similar to how the determinant of a matrix is determined, and that's why the wave function of this form is called slater determinant

$$\psi(r_1 ..., r_N) = \frac{1}{\sqrt{N!}} \begin{vmatrix} \varphi_1(r_1) & \cdots & \varphi_1(r_N) \\ \vdots & \cdots & \vdots \\ \varphi_N(r_1) & \cdots & \varphi_N(r_N) \end{vmatrix} \tag{3.20}$$

The determinant form helps to illustrate important properties of a many-particle wave function. Each line corresponds to a certain one- electron state, and each column to a certain position in space, among N positions $r_1, ..., r_N$ of particles we consider. The interchange of either two rows or two columns means that we interchanged two particles; the wave functions one then changes sign by construction.

Moreover, if there happen two identical lines or two identical columns, it means that two particles share the same spatial coordinates, the determinant then equals zero, meaning that such situation is physically impossible. Thus for arbitrary number of electrons the wave function form in above equation can be shown to satisfy the desire asymmetry condition. The determinant referred as a slater determinant, has N! term each multiplied by -1 and 1 depending on the parity of the permutation. For the calculation of energy eigenvalue, we now calculate the expectation value of Hamiltonian for this variational wave function[49].

3.1.4 Hohenberg and Kohn theorems

Hohenberg-Kohn (HK) reformulated the Schrodinger equation no longer in terms of wave functions but employing electron density, which can be defined for an N-electron system by:

$$\psi_e(r_1, r_2, ..., r_N) = \psi_e(r_1)\psi_e(r_2), ...\psi_e(r_N) \tag{3.21}$$

This equation depends only on the three position parameters r=(x, y, z), position vector of a given point in space. This approach is based on two theorems demonstrated by Hohenberg and Kohn.
Theorem1: For any system of interacting particles in an external potential $V_{ext}(\vec{r})$, the potential $V_{ext}(r)$ is only determined, except for an additive constant, by the electron density $n_o(r)$ in its ground state. The first HK Theorem can be demonstrated very simply by using reasoning by the absurd. Suppose there can be two different external potentials $V_{1ext} and V_{2ext}$ associated with the ground state density $n(\vec{r})$. These two potentials will lead to two different Hamiltonian $H_1 and H_2$ whose wave functions $\psi_1 and \psi_2$describing the ground state are different. As described by the ground state ofH_1we can therefore write that:

$$E_1 = \langle\psi_1|H_1|\psi_1\rangle < \langle\psi_2|H_1|\psi_2\rangle \tag{3.22}$$

This expression can be written as

$$E_1 = \langle\psi_1|H_1|\psi_1\rangle < \langle\psi_2|H_1|\psi_2\rangle \tag{3.23}$$

$$\langle\psi_2|H_1|\psi_2\rangle = \langle\psi_1|H_2|\psi_1\rangle + \langle\psi_2|H_1 - H_2|\psi_2\rangle \tag{3.24}$$

$$\langle\psi_2|H_1|\psi_2\rangle = E_2 + \int [V_{1ext}(\vec{r}) - V_{2ext}(\vec{r})]n_o(\vec{r})d^3(r) \tag{3.25}$$

$$E_1 < E_2 + \int [V_{1ext}(\vec{r}) - V_{2ext}(\vec{r})]n_o d^3(r) \tag{3.26}$$

$$E_1 + E_2 < E_1 + E_2 \tag{3.27}$$

It wills also the same reasoning can be achieved by considering E(2) instead of E(1). We then obtain the same equation as before, the symbols being inverted:

$$E_2 = \langle\psi_2|H_2|\psi_2\rangle < \langle\psi_1|H_1|\psi_1\rangle \tag{3.28}$$

$$\langle \psi_1 | H_2 | \psi_1 \rangle = \langle \psi_1 | H_1 | \psi_1 \rangle + \langle \psi_1 | H_2 - H_1 | \psi_1 \rangle \tag{3.29}$$

$$\langle \psi_1 | H_2 | \psi_1 \rangle = E_1 + \int [V_{2ext}(\vec{r}) - V_{1ext}(\vec{r})] n_o(\vec{r}) d^3(r) \tag{3.30}$$

$$E_2 < E_1 + \int [V_{2ext}(\vec{r}) - V_{1ext}(\vec{r})] n_o d^3(r) \tag{3.31}$$

$$E_1 + E_2 < E_1 + E_2 \tag{3.32}$$

The initial hypothesis is therefore false; there cannot exist two external potentials differing by more than one constant leading at the same density of a non-degenerate ground state. This completes the demonstration the external potential of the ground state is a density functional.

Theorem 2: The previous theorem only exposes the possibility of studying the system via density. It only allows knowledge of the density associated with the studied system. The Hohenberg-Kohn variation principle partially answers this problem: a universal functional for the energy E[n] can be defined in terms of the density. The exact ground state is the overall minimum value of this functional. Since the fundamental energy of the system is uniquely determined by its density, then energy can be written as a density functional. By following reasoning similar to that of the first part we show that the minimum of the functional corresponds to the energy of the ground state, indeed, the total energy can be written:

$$E_{Hk}[n] = \int n(\vec{r}) V_{ext}(\vec{r}) d^3 r + F_{Hk}[n] \tag{3.33}$$

F[n] is a universal functional of n(r)

$$F_{Hk}[n] = T[n] + V[n] \tag{3.34}$$

and the number of particles

$$N = \int n(\vec{r}) dr \tag{3.35}$$

Thus, we see that by minimizing the energy of the system with respect to the density we will obtain the energy and the density of the ground state. Despite all the efforts made to evaluate this functional E[n], it is important to note that no exact functional is yet known[50].

3.1.5 The Kohn-Sham equations

Since the kinetic energy of a gas of interacting electrons being unknown, in this sense, Walter Kohn and Lu Sham (KS) proposed in 1965 an ansatz which consists in replacing the system of electrons in interaction, impossible to solve analytically, by a problem of independent electrons evolving in an external potential. The Hohenberg- kohn theorems show that it is possible to use the ground state density to calculate the physical properties of a system. But it does not tell us a way to find the ground state density. The difficulty is overcome by the kohn-sham equation[51].the correlation energy is defined as part of the total energy absent in the Hartree-Fock solution. This motivates rewriting the total energy $E = T + V$ as

$$EV_{ext}[\rho] = T_0[\rho] + V_H[\rho] + V_{xc}[\rho] + V_{ext}[\rho] \tag{3.36}$$

where T_0, V_H, and V_{xc} are the kinetic energy, Hartree potential, and exchange correlation functional, respectively. The corresponding Hamiltonian is called the Kohn-Sham Hamiltonian

$$\hat{H}_{ks} = \hat{T}_0 + \hat{V}_H + \hat{V}_{xc} + \hat{V}_{ext} \tag{3.37}$$

The exchange-correlation potential is given by the functional derivative of the exact ground state density

$$\hat{V}_{xc} = \frac{\delta E_{xc}[\rho]}{\delta \rho} \tag{3.38}$$

The Kohn-Sham method is an exact description of the ground state properties of many-electron systems. However, the exchange-correlation functional is unknown and demands further approximations.

3.2 Density functional theory

Density functional theory is one of the most widely used methods for calculating the electronic structure of matter in both condensed matter physics and quantum chemistry. The DFT has become, over the last decades, a theoretical tool which has taken a very important place among the methods used for the description and the analysis of the physical and chemical properties for the complex systems, particularly for the systems containing a large number electrons.

DFT is a reformulation of the N-body quantum problem and as the name suggests, it is a theory that only uses electron density as the fundamental function instead of the wave function as is the case in the method by Hartree and Hartree - Fock. The principle within the framework of the DFT is to replace the function of the multi electronic wave with the electronic density as a base quantity for the calculations. The formalism of the DFT is based on the two theorems of Hohenberg and Kohn. It is one of the most popular, power full and successful quantum mechanical modeling methods used to investigate the electronic and structural property of materials.

The aims to describe the ground state property of many- electron system in terms of the electronic charge density. Used for calculation the binding energy of the molecules in chemistry, Also the electronic and phononic band structures of solids in physics,in the present thesis, DFT calculations are performed to investigate the electronic structure of nitrogen doped borophen. Density functional theory (DFT) is a quantum-mechanical atomistic simulation method to compute a wide variety of properties of almost any kind of atomic system: molecules, crystals, surfaces, and even electronic devices when combined.

DFT belongs to the family of first principles (ab initio) methods, so named because they can predict material properties for unknown systems without any experimental input. Among these, DFT has earned popularity due to the relatively low computational effort required. The DFT approach is widely applied in organic and inorganic chemistry, materials sciences like metallurgy or ceramics, and for electronic materials, to just name a few areas[52].

3.2.1 Exchange-correlation functional

As described above, DFT is at the stage of Kohn-Sham equations, a perfectly correct theory insofar as the electron density which minimizes the total energy is exactly the density of the

system of N interacting electrons. However, DFT remains inapplicable because the exchange-correlation potential remains unknown. It is therefore necessary to approximate this exchange-correlation potential. Two types of approximations exist the local density approximation or LDA and the generalized gradient approximation or GGA .

i. Local-Density Approximations (LDA)

Local density approximation is class of approximation to the exchange correlation energy functional in density functional theory (DFT) that depends solely up on the value of the electron density at each point in space (and not for example derivative of the density or the Kohn - Sham orbital). Many approaches can yield local approximation to the exchange energy . In general for a spin-un polarized system a local density approximation for the exchange- correlation energy [51]. In this approximation the exchange-correlation energy is compared to the homogeneous electron gas,

$$E_{xc}[n] = \int n(r)\varepsilon_{xc}[n]dr \tag{3.39}$$

Where n(r) is the electron density and ε_{xc} is the exchange correlation energy per particles of homogeneous electron gas of charge density. And also this, the exchange - correlation energy is decomposed in to exchange and correlation terms linearly

$$E_{xc} = E_x + E_c \tag{3.40}$$

The exchange term E_x and takes on a simple analytic form the homogenous electron gas. Local density approximation are important in the construction of more sophisticated approximation to the exchange - correlation energy. In general, the LDA approximation gives good results in describing the structural properties, i.e. it allows to determine the energy variations with the crystalline structure although it overestimates the cohesion energy, also concerning the mesh parameter for the majority of solids and good values of elastic constants like the isotropic modulus of comprehensibility. But this model remains insufficient in in-homogeneous systems.

ii. Generalized Gradient Approximations (GGA)

The exchange-correlation functional is written as a function of local density and the local gradient of the density. Also, as the LDA approximates the energy of true density by the energy of a local constant density. It fails in the situation where the density undergoes rapid changes such as in molecules. The logical step to go beyond LDA is the uses of not only the information about the density of electron, n(r)at a point r, but also to supplement the density with information about the gradient of density, (r) in order to account for the non-homogeneity of the true electron density. This approximation is called generalized gradient approximation (GGA)

$$E_{xc}^{GGA} = E_{xc}[n(r),(r)] \tag{3.41}$$

it can also

$$E_{xc}^{GGA}[n] = \int n(r)E_{xc}[\nabla n(r), n(r)]dr \tag{3.42}$$

In many cases the GGA improves the total energy, structural parameters and binding energies of molecules. The two sets of functional forms widely used in exchange correlation energy introduced respectively by Perdew and wang and Perdew, Burke and Ernzerhof in 1996(PBE)[53]. But in our calculation we used the GGA with PBE(PBE (Perdew-Burke-Ernzerhof). In general,Describing the electron exchange-correlation term is done within the generalized gradient approximation (GGA) in form of Perdew–Burke–Ernzerhof (PBE) correction

3.3 Quantum Espresso

Is a variety of numerical methods and algorithms aimed at a chemically realistic modeling of materials from the nano scale upwards, based on the solution of the density functional theory (DFT). It is an integrated suite of computer codes for electronic structure calculations and materials modeling based on DFT, plane waves and pseudo potentials (norm conserving, ultra soft and projector augmented wave) to represent the electron-ion interactions. The ESPRESS stands for open Source Package for Research in Electronic Structure, Simulation and optimization. The codes are constructed around the use of periodic boundary conditions, which allows for a straight forward treatment of infinite crystalline systems. Quantum espresso can do the following basic computations [54]
Density functional perturbation theory (DFPT), to calculate second and third derivatives of the total energy at any arbitrary wavelength. Ground state of magnetic or spin polarized systems.Atomic forces and stresses. Dynamical modeling (first-principles molecular dynamics) either on the electronic ground state (Born-Oppenheimer) or with fictitious electronic kinetic energy .Calculation of the Kohn-Sham (KS) orbitals and energies for isolated systems, and of their ground state energies. Complete structural optimizations of the microscopic(atomic coordinates) and macroscopic degrees of freedom.

3.3.1 Pseudopotential

In the pseudo-potential method for a solid, one considers the ion cores as a background in which the valence electrons move. These valence electrons actively participate in determining the chemical and physical properties of molecules and solids. This has led to the idea of the pseudo potential method: the interaction between the valence electrons and the ion core is treated with the pseudo potential which allows us to understand why the electron-ion core interaction is apparently so weak. The fact that pseudo-potentials are not unique allows the freedom to choose forms that simplify the calculations and the interpretation of the resulting electronic structure. The coulomb interaction is inversely proportional to the radial distance r. Because of this in the core region of the atom, potential becomes too large when electron is too close to core.

The wave functions of valance and core electrons have to be orthogonal. So that plane waves of these valance electrons are oscillating too much. To avoid this we can define a pseudo-potential. Instead of considering the potential of all core electrons, we can define a single pseudo potential which can describe the system with a good approximation. Due to this fact large energy cutoffs must be used to include plane waves that oscillate on short wave length scales in real space. This is problematic because the tightly bound core electrons in atoms are associated with wave functions with exactly this kind of oscillation. From a physical point of view, however, core electrons are not especially important in defining chemical bonding and other physical characteristics of materials; these properties are dominated by the less tightly bound valence electrons.

From the earliest developments of plane-wave methods, it was clear that there could be great advantages in calculations that approximated the properties of core electrons in a way that could reduce the number of plane waves necessary in a calculation. The most important approach to reducing the computational burden due to core electrons is to use pseudo-potentials. Conceptually, a pseudo-potential replaces the electron density from a chosen set of core electrons with

a smoothed density chosen to match various important physical and mathematical properties of the true ion core. The properties of the core electrons are then fixed in this approximate fashion in all subsequent calculations; this is the frozen core approximation. Calculations that do not include a frozen core are called all-electron calculations, and they are used much less widely than frozen core methods. Ideally, a pseudo-potential is developed by considering an isolated atom of one element, but the resulting pseudo potential can then be used reliably for calculations that place this atom in any chemical environment without further adjustment of the pseudo-potential. This desirable property is referred to as the transferability of the pseudo-potential. Current DFT codes typically provide a library of pseudo-potentials that includes an entry for each (or at least most) elements in the periodic table.

The details of a particular pseudo-potential define a minimum energy cut-off that should be used in calculations including atoms associated with that pseudopotential. Pseudopotentials requiring high cut-off energies are said to be hard, while more computationally efficient pseudopotentials with low cut-off energies are soft. The most widely used method of defining pseudopotentials is based on work by Vanderbilt; these are the ultra soft pseudo potentials (USPPs). As their name suggests, these pseudopotentials require substantially lower cut-off energies than alternative approaches. One disadvantage of using USPPs is that the construction of the pseudo-potential for each atom requires a number of empirical parameters to be specified. Current DFT codes typically only include USPPs that have been carefully developed and tested, but they do in some cases include multiple USPPs with varying degrees of softness for some elements. Another frozen core approach that avoids some of the disadvantages of USPPs is the projector augmented-wave (PAW) method originally introduced by Bloch and later adapted for plane-wave calculations by Kresse and Joubert. Kresse and Joubert performed an extensive comparison of USPP, PAW, and all electron calculations for small molecules and extended solids. Their work shows that well-constructed USPPs and the PAW method give results that are essentially identical in many cases and, just as importantly, these results are in good agreement with all-electron calculations. But in our calculation we used the USPP for as in the case of Boron is PBE-$\hat{V}_1$.4.USPP.F.UPF and in the nitrogen it has PBE-n-radius -5.UPF to used in the pseudopotentials

3.3.2 Bloch's theorems

An energy cut-off is used to fix the number of plane waves in the base set, rather than a straight forward option of choosing the number of plan waves as the former method ensures the reproduction of the optimal number of nodes when the cell size change, such as during a total cell relaxation. The energy cut-off for plane wave systems is usually tested by examining the convergence of energy difference between two like-systems.

$$\Psi_i(r) = e^{ik.r} g_i(r) \tag{3.43}$$

The Bloch's theorem can be stated as follows: in a periodic solid, the eigenvalues $\Psi_i(r)$ of an electron are given in the form of plane waves times the cell-periodic $g_i(r)$,

$$\Psi_i(r) = e^{ik.r} g_i(r) \tag{3.44}$$

The Bloch's theorem introduces wave vectors k which are always in the primitive cell of the reciprocal lattice and satisfy the expression $e^{ik.r} = 1$ for all lattice points. The potential $g_i(r)$ is

cell periodic and can be expressed as a fourier expansion of plane waves whose wave vectors are reciprocal lattice vectors of the crystal

$$g_i(r) = \sum_q C_i q e^{iq.r} \tag{3.45}$$

Where q is the reciprocal lattice vectors defined by the reciprocal of lattice vector ℓ as follows,

$$q.\ell = 2\pi n \tag{3.46}$$

and n is any integer. Now each electronic wave function can be expressed as the sum of all plane waves,

$$\Psi_i(r) = \sum_q c_{i,k+q} e^{i(q+k)r} \tag{3.47}$$

The $C_i, k+q$ are the coefficients for the plane waves that need to be solved and depend on the kinetic energy cut-off. The ECUT value determines the size of the plane wave basis set used to represent the electronic wave functions and significantly impacts both the accuracy and computational cost of the calculations. To determine the appropriate kinetic energy cutoff, we conducted convergence tests, with energy expressed in Rydberg (Ry). It is essential to set the energy cutoff sufficiently high to ensure that the total energy converges to the desired accuracy level. As the input energy increases, we observe that the total energy approaches to the horizontal ECUT value of that it demonstrating convergence. While increasing the energy cutoff generally leads to more accurate total energy calculations, it also results in higher computational costs

3.3.3 Plane wave

A plane wave is a wave who's the wave front are infinite parallel plans and it is parallel to the direction of propagation of the wave. These waves are plane and not spherical with increasing radius. Also plane wave are useful and simple for describing the electronic wave function in a periodic system. Because of this reason, to solve the Kohn-Sham equations, we expand the wave function at each k point in terms of plane wave basis. While doing this as a computational technique to simplify the calculation, we can use Fast Fourier Transformation (FFT). But it is impossible to make an expansion with infinite number of plane wave basis set. For this reason, we have to truncate our plane wave expansion. We can define an upper bound for the kinetic energy. Hence, we will only use plane waves which have less kinetic energy than our defined kinetic energy. In order to reduce errors we can increase the cut-off energy[55].

3.3.4 k-point sampling

The first Brillion zone can be mapped out by a continuous set of k-points throughout the region of reciprocal space. Represents the rectangular grid of points of dimensions k_x, k_y, k_z, spaced evenly throughout the Brillouin zone and this keyword requires appropriate unit. The k-point at which the Brillion zone is to be sampled during a self-consistent calculation to find the electronic ground-state may be defined either by specifying a list of k-points or a Monkhorst- pack grid in terms of the dimensions of the k-point mesh or a minimum k-point density[56].

These k-points represent the local where the electronic states are found in a solid system. If

there is an infinite number of electrons in a solid system there exists an infinite number of k-points in the Brillouin zone. In the calculation, the basis sets are required to represent the wave functions at a finite number of k-points. However, the basis sets calculations are still infinite even if the energy cut-off is chosen to be very small.

In the previous section, we discussed Bloch's theorem which enables us to consider a finite number of wave functions in the unit cell at an infinite number of k-points within the Brillouin zone. The electronic states calculated at a set of k- points contribute to the electronic potential of the solid system and are determined by the shape of the Brillouin zone. This is done since the electronic wave functions at the k-points that are close together will be identical, which causes the electronic wave functions to be represented over a region of reciprocal space at a single k-point. This enables us to calculate the electronic potential and the total energy of the solid system at a finite number of k-points. The error occurring during calculations can be made small by choosing a heavier set of k-points in the Brillouin zone. For example, in a metallic system, dense k-points are needed since it is very difficult to define the Fermi surface with a few points. The dense k-points still make the computational time lengthy and still offer a challenge in research [57]. And also, after this calculation of the cutoff energy value to fix that to make stability point from the graphe of cutoff energy from the amount of energy can be the same when we can take the value from the graphe in the horizontal Brillouin zone then, in order to perform the Brillouin zone interaction in discrete scheme. There is different large number of reading point used to by computational resources, we can optimize to calculate the total energy versus K-point. The point of dimension $K_x \times K_y \times K_z$ spaced evenly throughout the Brillouin zone is called K-point grid. We can estimate appropriate size by means of total energy calculation to approach the k-point sampling is suggested by Monkhrost and pack[56]. The total scf energy with different value of k-point grid is starting from $2 \times 2 \times 1$ to $16 \times 16 \times 1$ ranging between them. But from this work the material used be constant from $8 \times 8 \times 1$ that known as equilibrium point from the result of in our calculation we used in pristen the value of k-mesh $8 \times 8 \times 1$ and in super cell als we used $8 \times 8 \times 1$ and in the case of doping nitrogen for the concentration of x=0.33 we used the value of k-mesh of $6 \times 6 \times 1$ and also the when the amount of nitrogen doping of the concentration of x=0.38 we used the value of $5 \times 5 \times 1$ at the last work the amount of nitrogen doping concentration of x=0.44 we used $5 \times 5 \times 1$ in general.

3.3.5 Band structure

Band structures are a representation the allowed electronic energy levels of solid materials and used to better inform their electrical properties. A band structure is a 2D representation of the energies of the crystal orbital in a crystalline material. Sometimes referred to as "spaghetti diagrams" a band structure plot can quickly reveal whether a material is metallic, semi-metallic or insulating, and for those material with a band gaps whether they are direct or indirect as well as the magnitude of the gap. Additionally, the curvature of the bands can be reflecting the carrier mobility through those bands. While one is able to quickly determine many materials properties by examining a bond structure diagram, an intuitive understanding of how the band structures arise and why they are presented in such a ways requires deeper study.

The energy of the bands are calculated in "k-space" or sometimes called "momentum space".electronic structure calculation of crystals in the first principle electronic band structure is one of the most widely applied analytical tools especially with in the kohn -sham frame work of density functional theory calculation. Defferent electronic properties of solid are helpful to determine the

band structure of solids[24]. Because the lowest energy states are occupied by electrons, at 0K there is an energy below which all states are occupied, and above which all states are empty; this is the Fermi energy. Many band-structures are shifted so that the Fermi energy is at zero, but if not the Fermi energy will usually be marked clearly. In semi-conductors and insulators there is a region of energy just above the Fermi energy which has no bands in it this is called the band gap.

3.3.6 Density of state (DOS)

The density of states function describes the number of states that are available in a system and is essential for determining the carrier concentrations and energy distributions of carriers within a semiconductor. The density of state is commonly described in reciprocal space as a function of the state wave vector g(k), with the density of states being a count of the number of states in a given range of wave vector dk and the unit volume. The density of states is defined as the number of states per energy per unit volume of real space. It is easy to determine $g(\varepsilon)$ the total number of states per unit volume whose energy is less than ε and then obtain $g(\varepsilon)$ from it.

$$g(\varepsilon) = \frac{dN}{dE} \tag{3.48}$$

which is the number of states per unit volume in the range E to E + dE. Note that per unit volum refers to the space between intervals or points, and thus may be a length or area in lower dimensions. The density of states indicates the number of allowed states per unit of energy, and it can be used to express the orbital contribution of the participating atoms. Partial density of state (PDOS) is the relative contribution of a particular atom or orbital to the total dos. The results of partial density of states help to further elaborate the nature of band gap and gives information about the origin of bands. Density of states are calculated by pseudopotential and plan wave basis set method within the density functional theory. The results of density of states of B help to further elaborate the nature of the band gap.

3.3.7 Self consistency

Scf-is determines ground state electron density by calculating the energy difference with slightly changing the energy density. Consider the trial plane-wave function and the pseudo potential approach described in the KS equation. Although the solutions of KS equations provide the ground state charge density, they can not be taken as the desired results because one can obtain a more reliable and stable result by using the charge density which is achieved by iterating the solutions of KS equations. This method is called self-consistent field (SCF) approach. The self-consistent field (scf) calculations are performed to determine basic parameters:

i. kinetic energy cut-off for the plane wave basis and k-points grid by testing the convergence of total energy and calculation of lattice parameter by energy minimization.

ii. Define an initial, trial electron density, $n(r)$.

iii. Solve the Kohn Shame quations defined using the trial electron density to find the single-particle wave functions, $\psi(r)$.

iv. Calculate the electron density defined by the Kohn Sham single-particle wave functions from step iii, $n_{ks}(r)$.

Non-Self-Consistent field-it use

- It dos not require repeated evaluations of the Hamiltonian or Kohn-Sham operators
- Use full or large-scale simulations.

3.3.8 Convergence Tests

The self-consistent field(Scf) calculations are performed to determine basic parameters kinetic energy cut-off for the plane wave basis and k-points grid by testing the convergence of total energy and calculation of lattice parameter by energy minimization. BFGS (Broyden–Fletcher–Goldfarb–Shanno) is an iterative method used in computational optimization to find the minimum of a differentiable function. It is classified as a quasi-Newton method, which means it approximates the Newton's method for optimization but without requiring the computation of the Hessian matrix (second derivatives of the function).

Chapter 4

Result and Discussion

4.1 Geometric optimization and Electron structure of borophene

Geometric optimization is also known as structural optimization which is a crucial step in the computational modeling of electronic structures in materials. The unit cell of mono layer of borophene material compose B-B atom. Then the pristine unit cell of borophene is shown in the Figure 4.1.

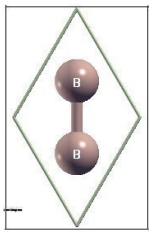

Figure 4.1: Pristine monolayer of Borophene Optimized constructed by using XcrysDen software.

In this study, the optimization process was carried out until the energy of the ground state atoms was minimized and the total energy of the system reached a local or global minimum. The calculations were conducted over a range of ground state energies, with values ranging from -12.25363813 Ry to -12.40513 Ry with corresponding ECUT value ranging from 12RY to 84RY. The total energy stabilized at -12.4051 Ry, with a corresponding cutoff energy (ECUT) of 51.9855 Ry. This indicates that the energy variations became significant no change after reaching 51.9855 Ry Figure 4.2. Convergence tests were conducted as shown on the Figure 4.2 and Figure 4.3 K-mesh respect to total energy. The reported value lattice parameter of borophene $(a = 1.61A^o)$,which is slightly larger than 4.4 its our value $(a = 1.6416A^o)$ in ref[58]. The percent difference between the two values is 1.975% indicating that our result is in good agreement with the reported value. This small difference suggests that the lattice parameter we obtained is consistent with existing data.

From the band structure of pristine show in Figure 4.5, the point where the conduction band and valance band touch each other are at a point $\wedge$" between [$\Gamma - M$] and at "K" high symmetric K-points. In the band structure diagram the Fermi energy levels crosses the bands, confirms the metallic property of the material. In Figure 4.6, the total density of state in conduction band reaches its peak value at 1.3eV at specific energy of 2.2eV, while in valance

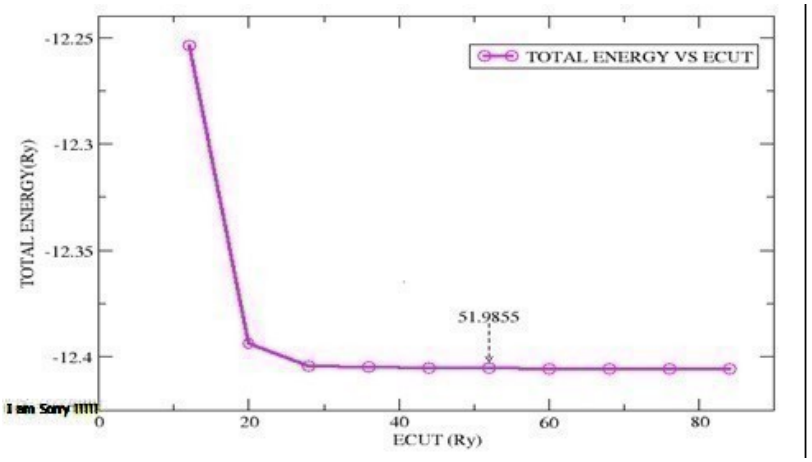

Figure 4.2: The graph of pristine monolayer of Borophene ECUT Structure Optimization

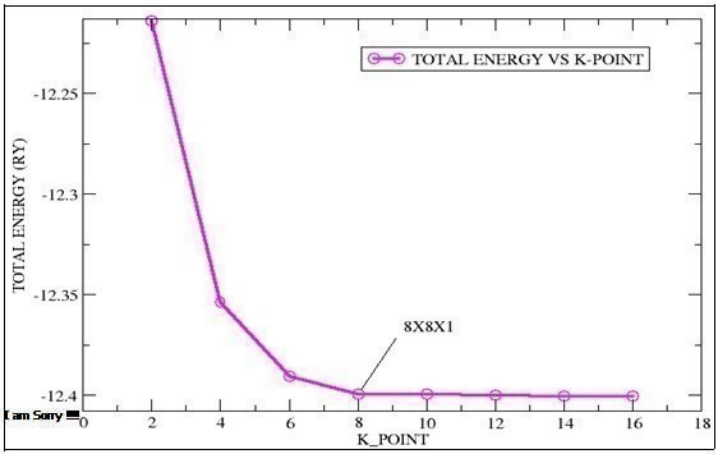

Figure 4.3: The graph of pristine k-point sampling Structure Optimization of mono layer of borophene

band it reaches maximum value 1eV at a specific energy level of -0.5eV. From band structure of TDOS of the material,our result agreed with, unlike many two-dimensional materials acting as semiconductor or semi-metal, borophene has a metallic property that has been reported in other papers [24].

4.2 Electronic Optimization of *h*-borophene super cell

For this thesis $3 \times 3 \times 1$ super cell that consistence eighteen (18) *h*-boron atoms, crucial for use in a doping system as shown Figure4.7. The band structures in the super cell indicate an increase in conductivity, reflecting a stronger metallic character. Because mobility of electron increase. The complexity of the band structure is evident, particularly as the band edges cross the Fermi level. This complexity increases with the number of boron atoms, as illustrated in Figure4.8.

Furthermore, the TDOS of the super cell, shown in Figure.4.9 indicates that the Fermi level is passed through highest peak of the total density of state,which shows the super cell has high-

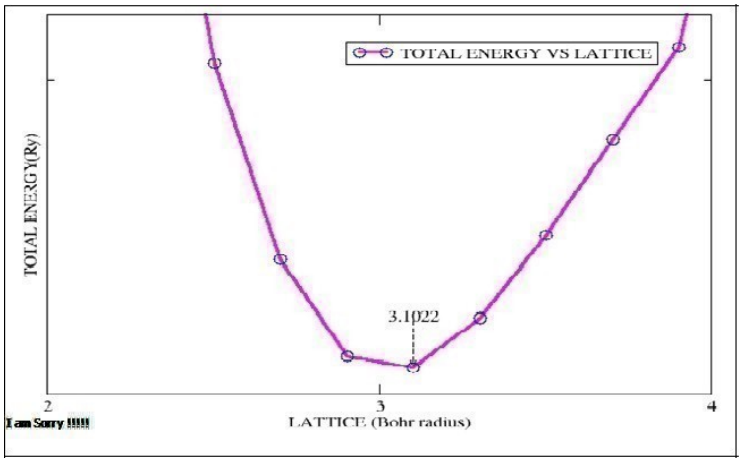

Figure 4.4: The graph of lattice parameter of borophene Optimization

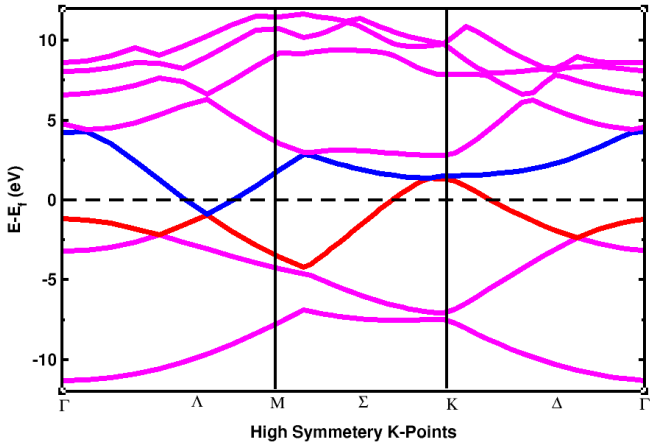

Figure 4.5: The graph of pristine band structure of borophene

est conductance than pristine.

From the Figure 4.9, the black line illustrates the total density of states (DOS) for the material. The projected density of states (PDOS) reveals that the 2s-orbital does not contribute to the conduction band, though it does make a minor contribution in the valence band. In contrast, the 2p-orbitals in the PDOS show significant presence across all energy levels, closely matching the overall TDOS in their contribution.

This analysis suggests a consistent gradient within the diagrams, especially around the Fermi level, as well as within the valence and conduction bands. This consistency strongly indicates high conductivity. By comparing the DOS with the band structure diagrams, we see a strong correlation between them.

It is clear from the partial density of states Figure 4.9 that the p orbital contribution high, and given that the s orbital contribution is very small, so it does not have a significant contribution to the metallic property and the main contribution is for the p orbital. In general, the contribution of the p orbital is greater than that of the s orbital, and accordingly, this orbital has a greater contribution in the electronic conduction.

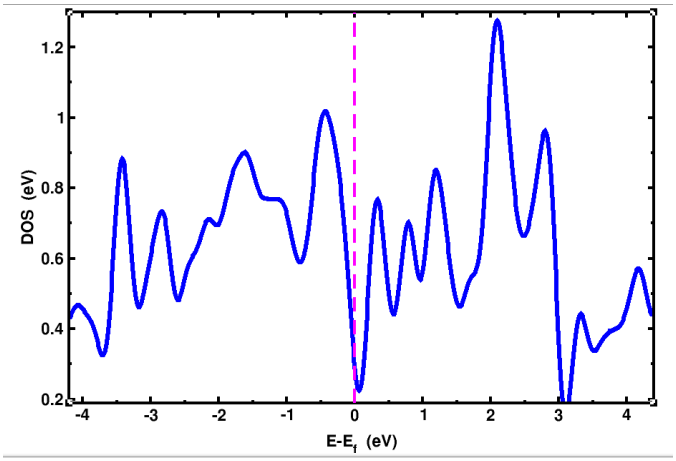

Figure 4.6: The graph of pristine total density of state for borophene

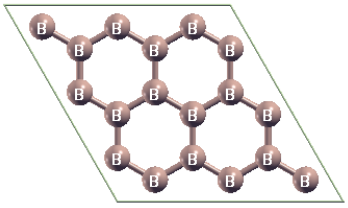

Figure 4.7: Monolayer hexagonal borophene (*h*-B) the optimized unit cell structure was replicated in x and y directions to get this $3 \times 3 \times 1$s super cell.

4.3 Electronic structure of nitrogen doped *h*-borophene

By introducing varying amounts of nitrogen into the *h*-borophene supercell, this study explores the possibility of changing *h*-borophene from a metallic to a semiconducting material. The impact of nitrogen doping on the electronic band structure and band gap of *h*-borophene examined and discussed in the following sections.

4.3.1 Nitrogen-Doped *h*-Borophene with concentration x=0.33

When six boron atoms as shown in the Figure 4.10 are substituted by nitrogen atom at concentration of x=0.33, the electron structure of the material altered. The band structure in Figure 4.11 shows that the bands opened from the left to right at$[\Gamma - \Delta]$, M and from $[\Delta - \Gamma]$. Furthermore, the edges of the conduction and valence bands it touch at two points$[\Delta - K]$. Unlike in the pristine band structure, the two points appear at the Fermi level, facilitating band opened at nitrogen concentration x=0.38. Once again, the two ends of the supercell band structure were closed at the Fermi energy level however, after six nitrogen atoms (6N) were doped, the two ends opened. From Figure 4.12 of the TDOS indicated by black color as will as PDOS show, as the material metallic characteristics. The conduction and valence bands are predominantly formed from the p-orbitals of boron atoms, with the s-orbital contribution from nitrogen atoms being undervalued. The s-orbital of the boron atom has a peak density of states value of 1.5 eV at an energy of -4 eV. However, in the conduction band, after 0.2 eV, it shows no significant value at all. Next to the p-orbital of the boron atom, the p- orbital of nitrogen plays a secondary role in building the valence band, but it contributes only slightly to the conduction band.

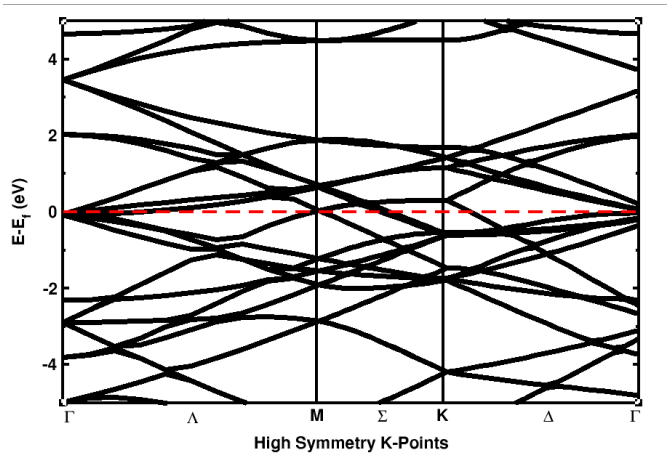

Figure 4.8: The band structure of super cell of *h*-borophene

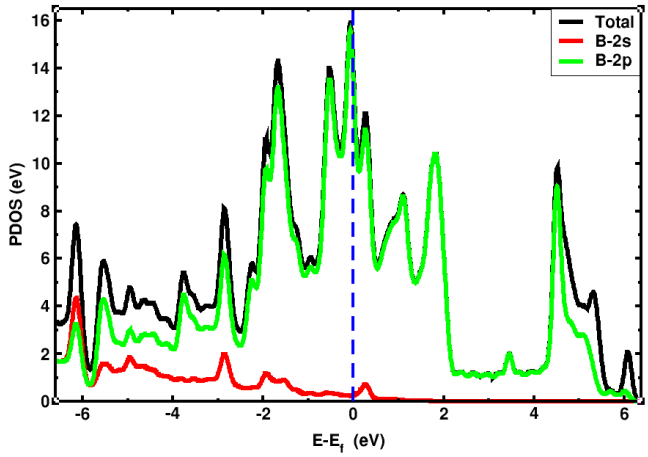

Figure 4.9: The super cell of TDOS and PDOS of mono layer of *h*- B

4.3.2 Nitrogen-Doped *h*-Borophene with concentration of x=0.38

Figure 4.13 illustrated that the increment of doping level of nitrogen atom concentration x=0.38 (7N).
The band gap of the material opened at a nitrogen doping level of x=0.38, with a small value of 0.5 eV, as illustrated in Figure 4.14. The maximum valence band was found at the symmetric point |Γ - Δ|, while the minimum conduction band edge was located at the symmetric point $|M - \sum|$, indicating the formation of a small, indirect band gap semiconductor.

This indirect band gap is defined by the separation between high-symmetry k-points, specifically $|\Gamma - \Sigma|$, indicating that the material is indirect band gap semiconductor because the valence and conduction band edges are located in different regions of the Brillouin zone. This difference in energy bands is illustrated in Figure 4.14. The gradients of the band structure diagram at the symmetric points $|\Gamma - M|$, |M-K|, and |k-Γ| support the above observations confirming that the gradient of the diagram, whether in the Fermi region or in the valence and conduction regions, indicates high conductivity.

The PDOS for the concentration of x=0.38 of nitrogen doped h-borophene in the conduction band it has high significance contribution it reaches its peak value at 8.2eV at a specific

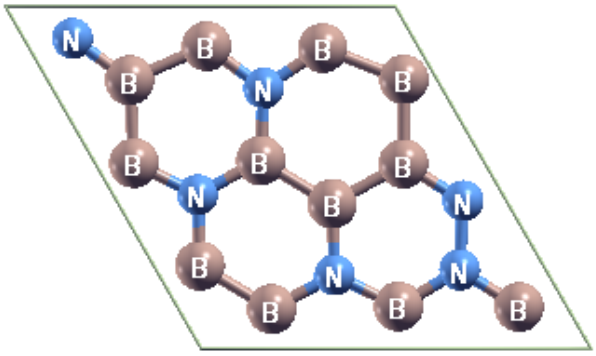

Figure 4.10: The pristine of nitrogen concentration x=0.33 of *h*-borophene Optimization

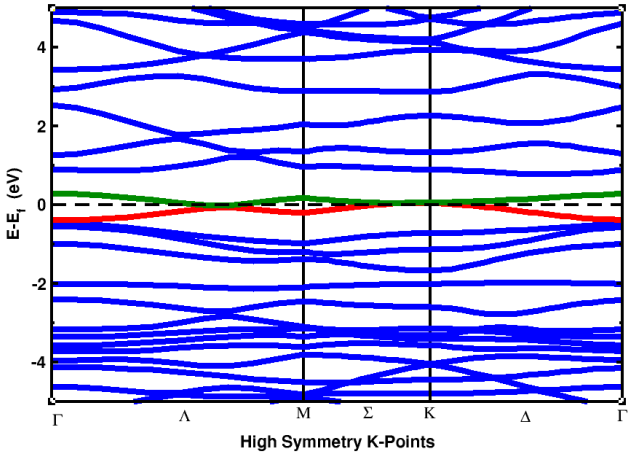

Figure 4.11: The band structure at the concentration of x=0.33 nitrogen doped *h*-borophene

energy of 0.25eV. And in the valance band the peak value it approach the Fermi level is at 6.8eV and a specific value of -0.25eV. However, the band edge it approach the Fermi level in the valance band when we compere with the conduction band. Overall, the total density of states (TDOS) reveals significant contributions from both the conduction and valence bands, with the valence band showing a notably higher contribution compared to the conduction band. For nitrogen-doped *h*- borophene at concentration of x=0.38, as illustrated in Figure 4.15, the total density of states indicates that the material is it has small band gap and in the valance band the band edge is it approach to the Fermi level. The total density of state from the Figure4.15 it shown the black line.

For nitrogen doping in *h*-borophene at a concentration of x=0.38, the projected density of states (PDOS) reveals that the 2s-orbital of boron contributes negligibly above 0.5 eV in the conduction band. On the other hand, the 2p-orbital of boron is found closest to the Fermi energy level in both bands, with a significant role in the development of both the conduction and valence bands, as illustrated in Figure 4.15.

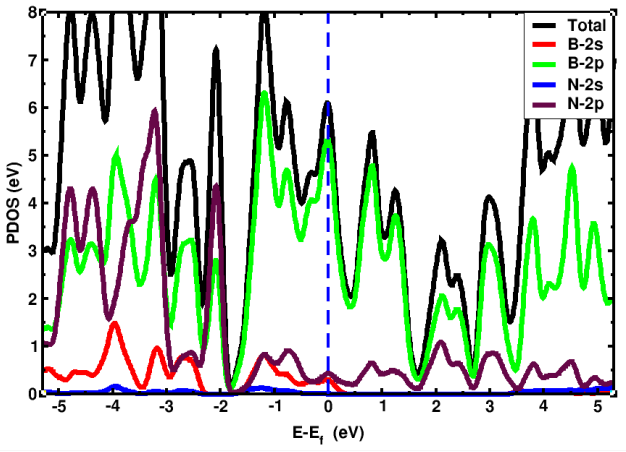

Figure 4.12: The total density of state and the pertial density of state for the concentration of x= 0.33 of nitrogen doped *h*-borophene

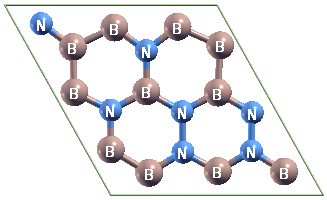

Figure 4.13: The super cells concentration of x=0.38 nitrogen doped *h*-borophene Optimized after relaxation.

4.3.3 Nitrogen-Doped *h*-Borophene with concentration of x=0.44

The system consists of a hexagonal unit cell of *h*-BN containing eighteen (18) atoms, which can be constructed using a $3 \times 3 \times 1$ K-point mesh within the super cell under periodic boundary conditions. In this configuration, 8 nitrogen (N) atoms are substituted into the borophene framework. The arrangement of the *h*-BN super cell, following the integration of nitrogen atoms into the borophene structure, is shown in Figure 4.16.

The consistency of this work the amount of concentration of nitrogen it increases from x=0.38 to x=o.44 the band gap it increases. We performed the electronic band structure and density of states along $\Gamma - M - K - \Gamma$ high symmetry directions to study the electronic properties of h-BN. The high-symmetry K-points in the grid are as follows:
$((0.0000at, \Gamma)(0.6540at, M), (0.9880at, K) and (1.5547at, \Gamma))$. From the band after performing structure calculations, we determined that the band gap of the material is 0.61 eV, indicating that this material has a direct band gap at the minimum point of the spectrum. This direct band gap is closest to the first Gamma (Γ) point at the origin, as shown in the graph of the band structure below Figure 4.17.

The other electrical property being analyzed is the total density of states (TDOS). When a nitrogen doping concentration of x= 0.44 is applied to the *h*-borophene sheet, the TDOS of the material is illustrated in Figure 4.18. In this graph, the black line represents the TDOS for a nitrogen doping concentration of x=0.44 on the *h*-borophene sheets. His contribution is it increases in both the conduction band and valance band. Overall, the density of states in both the conduction and valence bands is substantial, and at the zero Fermi level, the graph is open,then

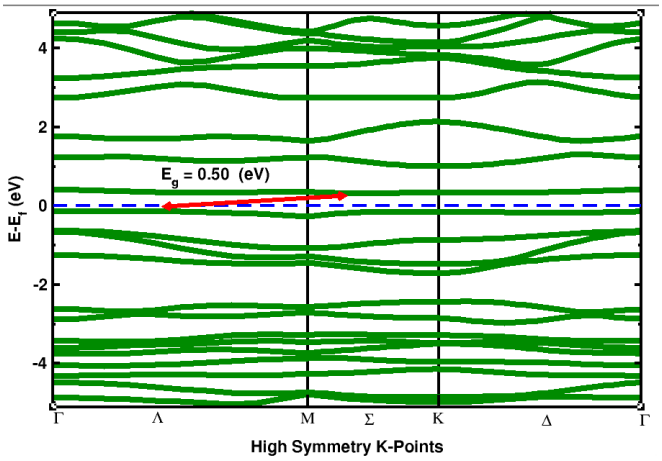

Figure 4.14: The band structure the concentration x=0.38 of nitrogen doped *h*-borophene

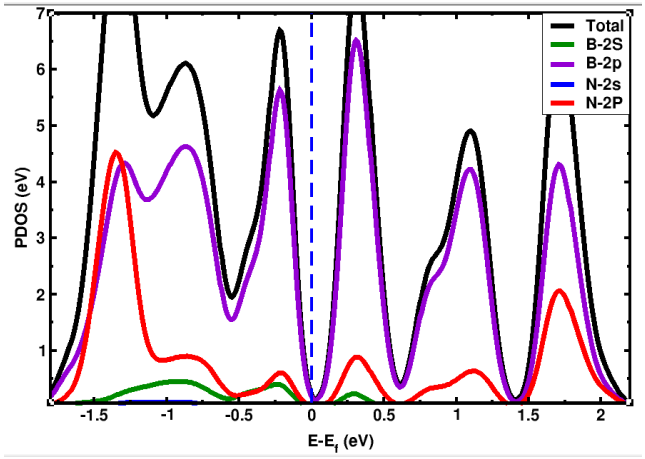

Figure 4.15: The total density of state and partial density of state concentration of x=0.38 nitrogen doped *h*-borophene

the valence band edge approaching the Fermi level.

Finally, the band edge near the Fermi level opens up, and in the valence region, the band edge approaches the Fermi level. The 2p orbitals of borophene play a crucial role in both the valence and conduction regions. And also when we compere the two PDOS on the concentration of x=0.38 Figure 4.15 and the concentration of x=0.44 Figure 4.18. It's important to note that the PDOS plays a critical role in identifying the distribution of electron states, which is essential for understanding the material's electronic properties. Additionally, when analyzing the PDOS graphs, we observe that the valleys occur at the same points from the concentration x=0.44 at the all orbital it shown in the Figure 4.18.

The consistency of this work we conclude that from the concentration of x=0.38 and x=0.44 nitrogen doped *h*- borophene from the material it has a small narrow band edge and the band edge of Fermi energy no cross each other but it touch one to the other. However, the band gap is very narrow and also the material is a P-type semiconductor.But the P type semiconductor are an accepter. By comparing the density of states and the band structure diagrams, a good agreement between them can be observed.

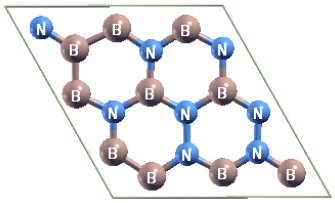

Figure 4.16: The super cells the concentration of x=044 nitrogen doped *h*-borophene optimization after relaxation.

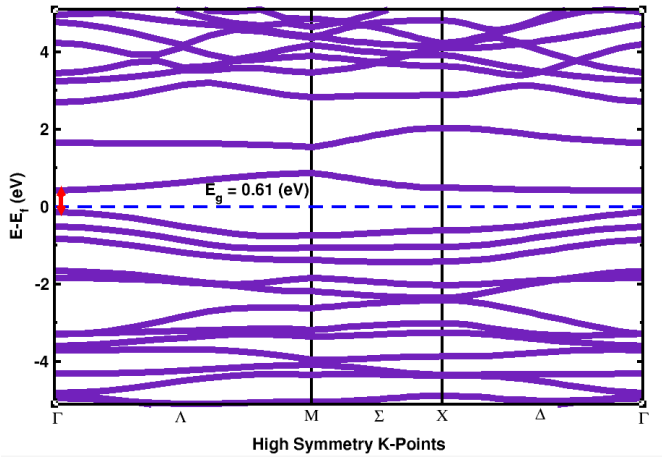

Figure 4.17: The band structure at the concentration of x=0.44 nitrogen doped *h*-borophene

what we conclude from this result for the concentration of x= 0.44 nitrogen doping further increasing the nitrogen concentration the results in a direct band gap of 0.61 eV referee to Figure 4.17 which is near to the Gamma (Γ) point. The material remains a P-type semiconductor with a narrow band gap. The band, TDOS and PDOS indicates that the 2p orbitals of both boron and nitrogen are vital in defining the material's electronic properties, particularly near the Fermi level.

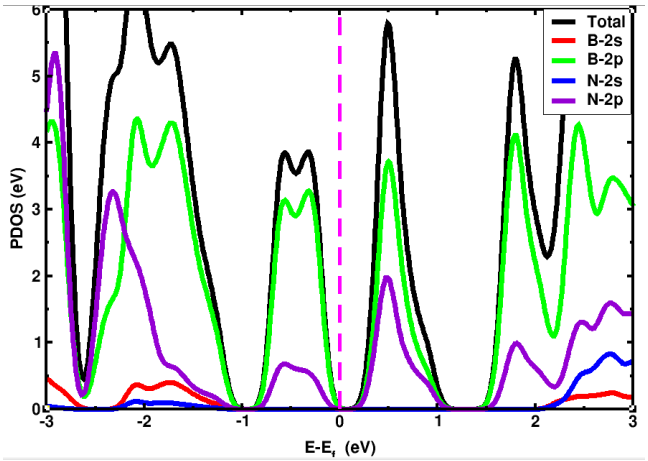

Figure 4.18: The total density of state and partial density of state for the concentration of x=044 nitrogen substitution *h*-borophene

Chapter 5

Conclusion and Recommendation For Future Work

- This paper conducted first-principle calculations to investigate the electronic structure of nitrogen-doped *h*-borophene to search for semiconductor materials.
- In our calculation, the electron structure of pristine borophene, its TDOS, and PDOS as well as band structure reveal that metallic properties.
- From our calculation, the $3 \times 3 \times 1$ super cell and nitrogen doped *h*-borophene at the concentration of x=0.33 possess band gapless and behaves as a metal.
- We found that,at nitrogen doped concentration of x=0.38 the band of *h*-borophene begin to opend by having indirect band at high symmetry point Λ-M and M-$\sum$
- As the nitrogen concentration increases to x=0.44, the increased band gap value of 0.61 eV, with the material maintaining a direct band gap, showing consistent behavior in its band structure as nitrogen dopant concentration increases.
- In this study,at the concentration of x=0.38 and x=0.44 nitrogen doped *h*-borophene the Fermi energy level found near the valance band edge, suggesting that the material behaves as p-type semiconductor
- We understood the possibility of altering *h*-borophene metal to semiconductor material by doping nitrogen at different concentration in order to use in semiconductor technology
- Future research should focus on an in-depth exploration of the electronic, optical, and magnetic properties of nitrogen-doped h-borophene, with particular emphasis on charge density calculations and the impact of nitrogen doping on physical characteristics.

Bibliography

[1] Mikhail I Katsnelson. Graphene: carbon in two dimensions. *Materials today*, 10(1-2):20–27, 2007.

[2] Ankur Gupta, Tamilselvan Sakthivel, and Sudipta Seal. Recent development in 2d materials beyond graphene. *Progress in Materials Science*, 73:44–126, 2015.

[3] Jeongteak Kwon and Jungyoon Kim. Fabrication and properties of pn diodes with hybrid 2d layers: Graphene/mos2. *Materials Express*, 8(3):299–303, 2018.

[4] Wen-cai Yi, Wei Liu, Jorge Botana, Lei Zhao, Zhen Liu, Jing-yao Liu, and Mao-sheng Miao. Honeycomb boron allotropes with dirac cones: a true analogue to graphene. *The Journal of Physical Chemistry Letters*, 8(12):2647–2653, 2017.

[5] Jianwen Yu, Ming Zhou, Mingyang Yang, Qingfeng Yang, Zhixun Zhang, and Yibo Zhang. High-performance borophene/graphene heterostructure anode of lithium-ion batteries achieved via controlled interlayer spacing. *ACS Applied Energy Materials*, 3(12):11699–11705, 2020.

[6] Bo Peng, Hao Zhang, Hezhu Shao, Yuanfeng Xu, Rongjun Zhang, and Heyuan Zhu. The electronic, optical, and thermodynamic properties of borophene from first-principles calculations. *Journal of Materials Chemistry C*, 4(16):3592–3598, 2016.

[7] Yinchang Zhao, Shuming Zeng, and Jun Ni. Superconductivity in two-dimensional boron allotropes. *Physical Review B*, 93(1):014502, 2016.

[8] Showkat H Mir, Sudip Chakraborty, Prakash C Jha, John Wärnå, Himadri Soni, Prafulla K Jha, and Rajeev Ahuja. Two-dimensional boron: Lightest catalyst for hydrogen and oxygen evolution reaction. *Applied Physics Letters*, 109(5), 2016.

[9] Dmitri Golberg, Yoshio Bando, Yang Huang, Takeshi Terao, Masanori Mitome, Chengchun Tang, and Chunyi Zhi. Boron nitride nanotubes and nanosheets. *ACS nano*, 4(6):2979–2993, 2010.

[10] RH Wentorf Jr. Cubic form of boron nitride. *The Journal of Chemical Physics*, 26(4):956–956, 1957.

[11] Zhuhua Zhang, Evgeni S Penev, and Boris I Yakobson. Two-dimensional boron: structures, properties and applications. *Chemical Society Reviews*, 46(22):6746–6763, 2017.

[12] Ihsan Boustani. New quasi-planar surfaces of bare boron. *Surface science*, 370(2-3):355–363, 1997.

[13] Clifford M Krowne and Xianwei Sha. Ab initio physics calculations for borophene for electronic devices. *arXiv preprint arXiv:2012.07582*, 2020.

[14] Meysam Makaremi, Bohayra Mortazavi, and Chandra Veer Singh. 2d hydrogenated graphene-like borophene as a high capacity anode material for improved li/na ion batteries: A first principles study. *Materials today energy*, 8:22–28, 2018.

[15] Yang Zhang, Zhi-Feng Wu, Peng-Fei Gao, Sheng-Li Zhang, and Yu-Hua Wen. Could borophene be used as a promising anode material for high-performance lithium ion battery? *ACS applied materials & interfaces*, 8(34):22175–22181, 2016.

[16] Yao Yao, Hongtao Yu, Yanan Wu, Yao Lu, Ziwei Liu, Xin Xu, Ben Ma, Qing Zhang, Shufen Chen, and Wei Huang. Efficient quantum dot light-emitting diodes based on trioctylphosphine oxide-passivated organometallic halide perovskites. *ACS omega*, 4(5):9150–9159, 2019.

[17] Xiuyun Zhang, John Xin, and Feng Ding. The edges of graphene. *Nanoscale*, 5(7):2556–2569, 2013.

[18] Cory R Dean, Andrea F Young, Inanc Meric, Chris Lee, Lei Wang, Sebastian Sorgenfrei, Kenji Watanabe, Takashi Taniguchi, Phillip Kim, Kenneth L Shepard, et al. Boron nitride substrates for high-quality graphene electronics. *Nature nanotechnology*, 5(10):722–726, 2010.

[19] S Cao. J. low, j. yu and m. jaroniec. *Adv. Mater*, 27:2150, 2015.

[20] Baojie Feng, Jin Zhang, Qing Zhong, Wenbin Li, Shuai Li, Hui Li, Peng Cheng, Sheng Meng, Lan Chen, and Kehui Wu. Experimental realization of two-dimensional boron sheets. *Nature chemistry*, 8(6):563–568, 2016.

[21] Qing Zhong, Jin Zhang, Peng Cheng, Baojie Feng, Wenbin Li, Shaoxiang Sheng, Hui Li, Sheng Meng, Lan Chen, and Kehui Wu. Metastable phases of 2d boron sheets on ag (1 1 1). *Journal of Physics: Condensed Matter*, 29(9):095002, 2017.

[22] Wenbin Li, Shaoxiang Sheng, Jian Chen, Peng Cheng, Lan Chen, and Kehui Wu. Ordered chlorinated monolayer silicene structures. *Physical Review B*, 93(15):155410, 2016.

[23] Dongchao Wang, Li Chen, Xiaoli Wang, Guangliang Cui, and Pinhua Zhang. The effect of substrate and external strain on electronic structures of stanene film. *Physical Chemistry Chemical Physics*, 17(40):26979–26987, 2015.

[24] Andrew J Mannix, Xiang-Feng Zhou, Brian Kiraly, Joshua D Wood, Diego Alducin, Benjamin D Myers, Xiaolong Liu, Brandon L Fisher, Ulises Santiago, Jeffrey R Guest, et al. Synthesis of borophenes: Anisotropic, two-dimensional boron polymorphs. *Science*, 350(6267):1513–1516, 2015.

[25] Xinming Li, Li Tao, Zefeng Chen, Hui Fang, Xuesong Li, Xinran Wang, Jian-Bin Xu, and Hongwei Zhu. Graphene and related two-dimensional materials: Structure-property relationships for electronics and optoelectronics. *Applied Physics Reviews*, 4(2), 2017.

[26] Lin Zhang, Pei Liang, Hai-bo Shu, Xiao-lei Man, Feng Li, Jie Huang, Qian-min Dong, and Dong-liang Chao. Borophene as efficient sulfur hosts for lithium–sulfur batteries: suppressing shuttle effect and improving conductivity. *The Journal of Physical Chemistry C*, 121(29):15549–15555, 2017.

[27] L Boldrin, F Scarpa, Rajib Chowdhury, and Sondipon Adhikari. Effective mechanical properties of hexagonal boron nitride nanosheets. *Nanotechnology*, 22(50):505702, 2011.

[28] Zhuhua Zhang, Yang Yang, Guoying Gao, and Boris I Yakobson. Inside back cover: Two-dimensional boron monolayers mediated by metal substrates (angew. chem. int. ed. 44/2015). *Angewandte Chemie International Edition*, 54(44):13135–13135, 2015.

[29] Zhuhua Zhang, Yang Yang, Evgeni S Penev, and Boris I Yakobson. Elasticity, flexibility, and ideal strength of borophenes. *Advanced Functional Materials*, 27(9):1605059, 2017.

[30] Jie Yang, Ruge Quhe, Shenyan Feng, Qiaoxuan Zhang, Ming Lei, and Jing Lu. Interfacial properties of borophene contacts with two-dimensional semiconductors. *Physical Chemistry Chemical Physics*, 19(35):23982–23989, 2017.

[31] Xiaolong Liu, Luqing Wang, Shaowei Li, Matthew S Rahn, Boris I Yakobson, and Mark C Hersam. Geometric imaging of borophene polymorphs with functionalized probes. *Nature communications*, 10(1):1642, 2019.

[32] Haifeng Wang, Qingfang Li, Yan Gao, F Miao, Xiang-Feng Zhou, and XG Wan. Strain effects on borophene: ideal strength, negative possion's ratio and phonon instability. *New Journal of Physics*, 18(7):073016, 2016.

[33] Cai Cheng, Jia-Tao Sun, Hang Liu, Hui-Xia Fu, Jin Zhang, Xiang-Rong Chen, and Sheng Meng. Suppressed superconductivity in substrate-supported $\beta 12$ borophene by tensile strain and electron doping. *2D Materials*, 4(2):025032, 2017.

[34] Liangzhi Kou, Yandong Ma, Liujiang Zhou, Ziqi Sun, Yuantong Gu, Aijun Du, Sean Smith, and Changfeng Chen. High-mobility anisotropic transport in few-layer γ-b 28 films. *Nanoscale*, 8(48):20111–20117, 2016.

[35] Hangbo Zhou, Yongqing Cai, Gang Zhang, and Yong-Wei Zhang. Superior lattice thermal conductance of single-layer borophene. *npj 2D Materials and Applications*, 1(1):14, 2017.

[36] Hongling Li, Lin Jing, Wenwen Liu, Jinjun Lin, Roland Yingjie Tay, Siu Hon Tsang, and Edwin Hang Tong Teo. Scalable production of few-layer boron sheets by liquid-phase exfoliation and their superior supercapacitive performance. *Acs Nano*, 12(2):1262–1272, 2018.

[37] Suleyman Er, Gilles A de Wijs, and Geert Brocks. Dft study of planar boron sheets: a new template for hydrogen storage. *The Journal of Physical Chemistry C*, 113(43):18962–18967, 2009.

[38] Xiaoyuan Ji, Na Kong, Junqing Wang, Wenliang Li, Yuling Xiao, Silvia Tian Gan, Ye Zhang, Yujing Li, Xiangrong Song, Qingqing Xiong, et al. A novel top-down synthesis of ultrathin 2d boron nanosheets for multimodal imaging-guided cancer therapy. *Advanced Materials*, 30(36):1803031, 2018.

[39] Anindya Das, AK Sood, Prabal K Maiti, Mili Das, R Varadarajan, and CNR Rao. Binding of nucleobases with single-walled carbon nanotubes: Theory and experiment. *Chemical Physics Letters*, 453(4-6):266–273, 2008.

[40] Aleksey Falin, Qiran Cai, Elton JG Santos, Declan Scullion, Dong Qian, Rui Zhang, Zhi Yang, Shaoming Huang, Kenji Watanabe, Takashi Taniguchi, et al. Mechanical properties of atomically thin boron nitride and the role of interlayer interactions. *Nature communications*, 8(1):15815, 2017.

[41] Roman V Gorbachev, Ibtsam Riaz, Rahul R Nair, Rashid Jalil, Liam Britnell, Branson D Belle, Ernie W Hill, Kostya S Novoselov, Kenji Watanabe, Takashi Taniguchi, et al. Hunting for monolayer boron nitride: optical and raman signatures. *arXiv preprint arXiv:1008.2868*, 2010.

[42] Jiangtao Wu, Baolin Wang, Yujie Wei, Ronggui Yang, and Mildred Dresselhaus. Mechanics and mechanically tunable band gap in single-layer hexagonal boron-nitride. *Materials Research Letters*, 1(4):200–206, 2013.

[43] Hokyeong Jeong, Dong Yeong Kim, Jaewon Kim, Seokho Moon, Nam Han, Seung Hee Lee, Odongo Francis Ngome Okello, Kyung Song, Si-Young Choi, and Jong Kyu Kim. Wafer-scale and selective-area growth of high-quality hexagonal boron nitride on ni (111) by metal-organic chemical vapor deposition. *Scientific reports*, 9(1):5736, 2019.

[44] Ayaka Yamanaka and Susumu Okada. Energetics and electronic structure of h-bn nanoflakes. *Scientific reports*, 6(1):30653, 2016.

[45] Wei Hu, Jingge Ju, Nanping Deng, Mengyao Liu, Weicui Liu, Yixuan Zhang, Lanlan Fan, Weimin Kang, and Bowen Cheng. Recent progress in tackling zn anode challenges for zn ion batteries. *Journal of Materials Chemistry A*, 9(46):25750–25772, 2021.

[46] Byung-Hyun Yun, Kyeong Joon Kim, Dong Woo Joh, Munseok S Chae, Jong Jun Lee, Dae-won Kim, Seokbeom Kang, Doyoung Choi, Seung-Tae Hong, and Kang Taek Lee. Highly active and durable double-doped bismuth oxide-based oxygen electrodes for reversible solid oxide cells at reduced temperatures. *Journal of Materials Chemistry A*, 7(36):20558–20566, 2019.

[47] A Sumiyoshi, H Hyodo, Y Sato, M Terauchi, and K Kimura. Good reproductive preparation method of li-intercalated hexagonal boron nitride and transmission electron microscopy–electron energy loss spectroscopy analysis. *Solid State Sciences*, 47:68–72, 2015.

[48] Margaret Czerw. *Computational studies of transition metal complexes relevant to catalytic alkane functionalization*. Rutgers The State University of New Jersey, School of Graduate Studies, 2004.

[49] Attila Szabo and Neil S Ostlund. *Modern quantum chemistry: introduction to advanced electronic structure theory*. Courier Corporation, 2012.

[50] A Nagy. Relativistic density-functional theory for ensembles of excited states. *Physical Review A*, 49(4):3074, 1994.

[51] Walter Kohn and Lu Jeu Sham. Self-consistent equations including exchange and correlation effects. *Physical review*, 140(4A):A1133, 1965.

[52] Kyle A Baseden and Jesse W Tye. Introduction to density functional theory: Calculations by hand on the helium atom. *Journal of chemical education*, 91(12):2116–2123, 2014.

[53] John P Perdew, Kieron Burke, and Matthias Ernzerhof. Generalized gradient approximation made simple. *Physical review letters*, 77(18):3865, 1996.

[54] Reiner M Dreizler and Eberhard KU Gross. *Density functional theory: an approach to the quantum many-body problem*. Springer Science & Business Media, 2012.

[55] Mike C Payne, Michael P Teter, Douglas C Allan, TA Arias, and ad JD Joannopoulos. Iterative minimization techniques for ab initio total-energy calculations: molecular dynamics and conjugate gradients. *Reviews of modern physics*, 64(4):1045, 1992.

[56] James D Pack and Hendrik J Monkhorst. " special points for brillouin-zone integrations"—a reply. *Physical Review B*, 16(4):1748, 1977.

[57] Refilwe Edwin Mapasha et al. *Theoretical studies of graphene and graphene-related materials involving carbon and silicon*. PhD thesis, University of Pretoria, 2011.

[58] Jesús Carrete, Wu Li, Lucas Lindsay, David A Broido, Luis J Gallego, and Natalio Mingo. Physically founded phonon dispersions of few-layer materials and the case of borophene. *Materials Research Letters*, 4(4):204–211, 2016.